UCID-21371

ESTIMATION OF BALLOON POSITION FROM WIND DATA

Lawrence C. Ng

Michael F. Kelly

March 1988

Lawrence Livermore National Laboratory

Work performed under the auspices of the U.S. Department of Energy by the Lawrence Livermore National Laboratory under Contract W-7405-Eng-48.

Printed in the United States of America
Available from
National Technical Information Service
U.S. Department of Commerce
5285 Port Royal Road
Springfield, VA 22161

Price Code	Page Range
A01	Microfiche
Papercopy Prices	
A02	001 - 050
A03	051 - 100
A04	101 - 200
A05	201 - 300
A06	301 - 400
A07	401 - 500
A08	501 - 600
A09	601

Table of Contents

ESTIMATION OF BALLOON POSITION FROM WIND DATA

Lawrence C. Ng

Michael F. Kelly

Abstract

The report summarizes the mathematical algorithm and the computed results developed for the prediction of a balloon's position uncertainty as a function of time from a given statistical wind velocity profile. The predicted results were used for mission plannings in support of a recent ship launch balloon observation experiment.

Administrative Information

This work was conducted under account number 6823-06, the PROBE project, the principal investigator is Cliff Chocol. The authors of this report are located at the Lawrence Livermore National Laboratory.

Acknowledgment

The authors wish to express their appreciation for contributions made by Fran McFarland in the preparation of this report.

1. Problem Description and Formulation

An observation balloon equipped with appropriate instrumentation package is to be launched from a ship. At the termination of the observation period (normally less than two hours), the instrumentation package will be released from the balloon *via* remote control and subsequently recovered. Throughout the observation experiment, the exact location and altitudes of the balloon will be tracked. However, for planning purposes, it is required to estimate the balloon's flight trajectory such that a launch position sufficiently far in the upwind direction can be determined. Subsequently when the instrument package is to be released, it will impact at sea rather than on land. Furthermore since the recovery of the instrumentation package is to be carried out by a helicopter stationed at a nearby island, it is desired to have the release point located as near as possible to the helicopter station. This situation is depicted in Figure 1.

Prediction of a balloon's flight is complicated by the wind motion uncertainty; its velocity changes in both magnitude and direction as a function of altitudes. Figure 2 shows a typical wind velocity profile. Its statistical nature was derived from many repeated meterological observations. Assuming that the balloon follows the wind motion, one can then derive a relative simple prediction algorithm. This result will be useful for the purpose of determining the balloon's launch position.

Mathematical Formulation

Figure 3 depicts the kinematic of the balloon motion and the orientation of the reference coordinates. Referring to Figure 4, the following notations were used.

An x, y, z rectangular coordinate system whose origin coincides with the launch point is defined as follows: x – points east, y – points north, and z – points up. Furthermore, the wind velocity is denoted by w, the horizontal component, u, the vertical component, and θ it s direction with respect to (w.r.t) the x axis (*i.e.*, easterly direction). For a wind arrival direction ψ, which is measured clockwise w.r.t north, (a convention used in the meterological database), θ and ψ are related by

$$\theta = \psi - 270^\circ \quad . \tag{1}$$

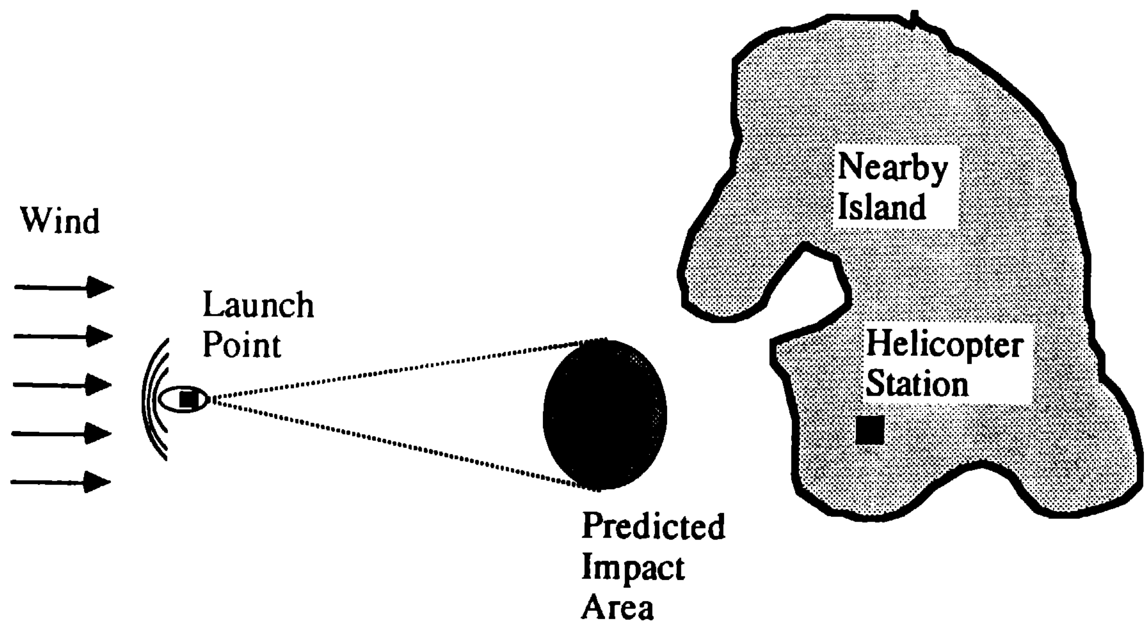

Figure 1. Geometry for balloon experiement and instrumentation package recovery.

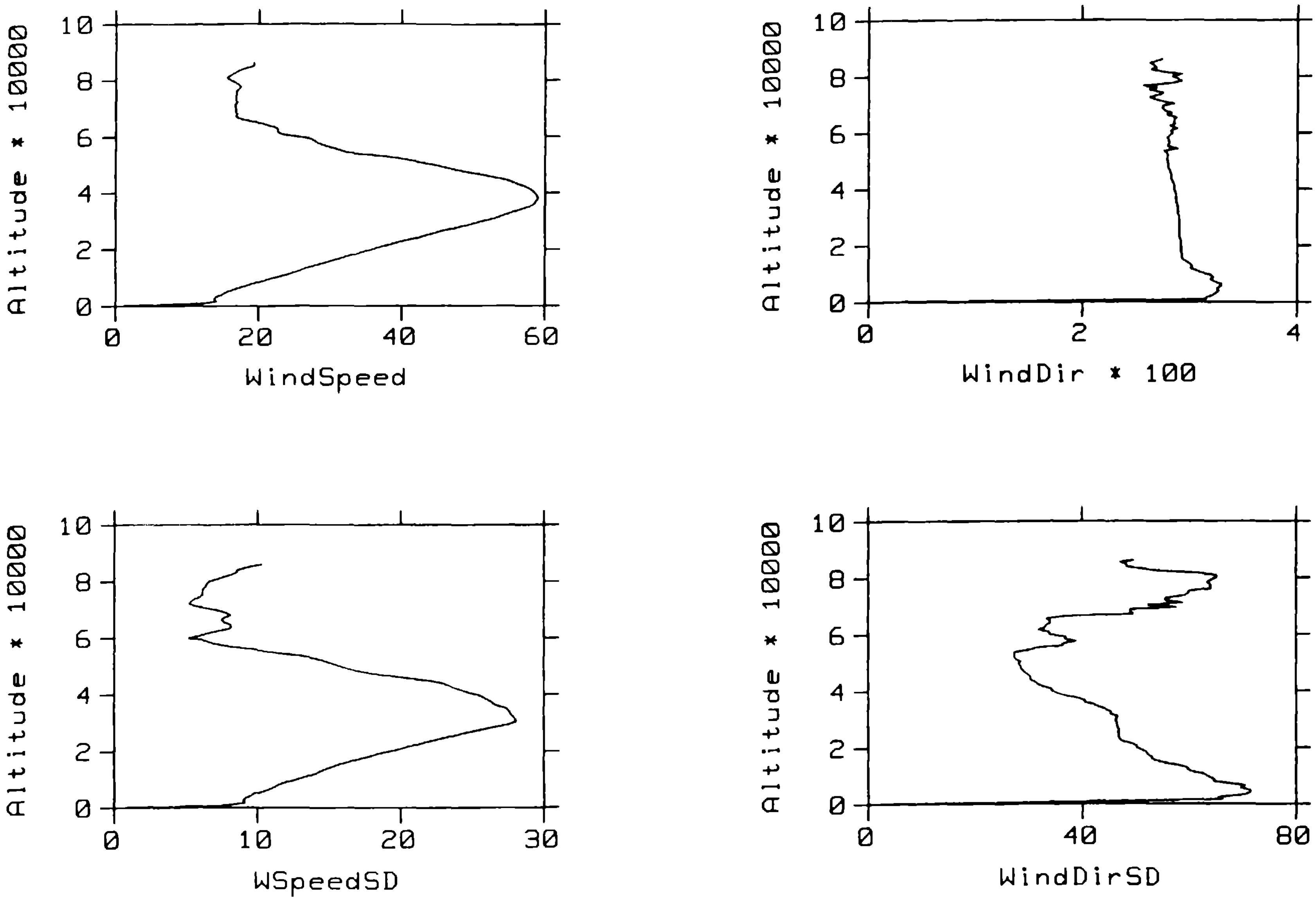

Figure 2. Altitude in feet, wind speed in knots, wind direction in degrees clockwise from North, weather data from San Nicholas Island typical for the month of February.

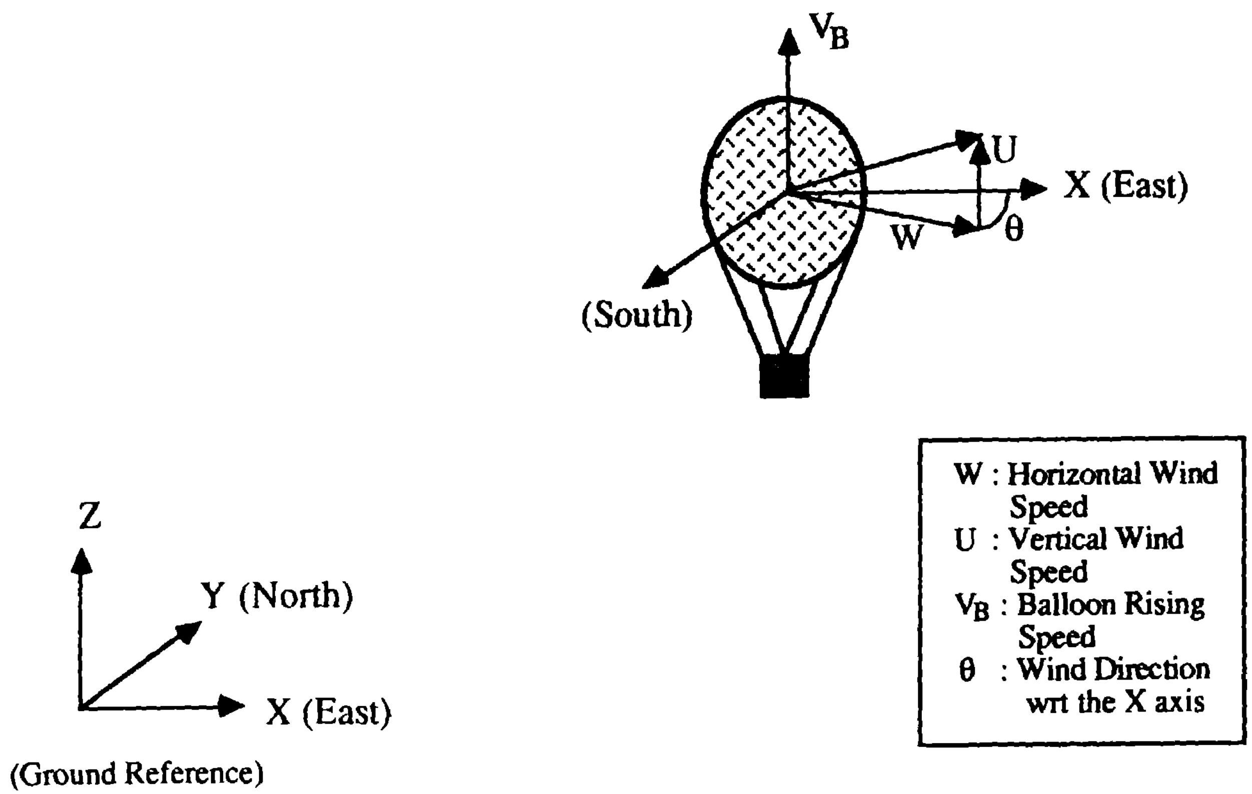

Figure 3. Balloon kinematrics and coordinate references.

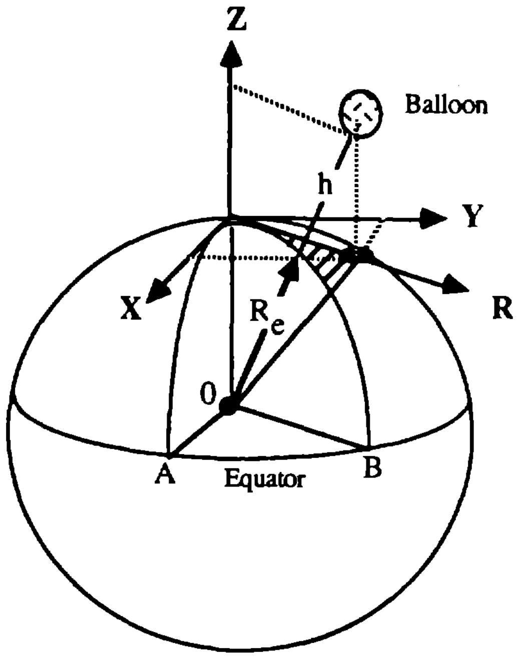

Figure 4a. Balloon altitudes expressed as a function of X, Y, and Z.

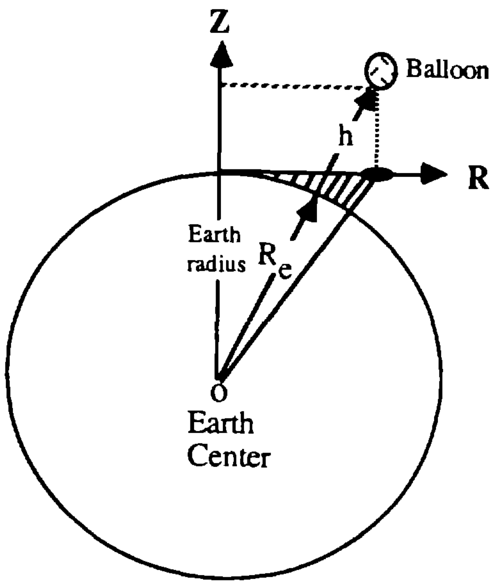

Figure 4b. Balloon altitudes expressed as a function of R and Z.

Defining V_B as the balloon ascent speed in zero vertical wind speed conditions then the balloon velocity at any time after launch can be described by the differential equations

$$\begin{aligned}\dot{x}(t) &= w(h)\cos\theta(h)\\ \dot{y}(t) &= w(h)\sin\theta(h)\\ \dot{z}(t) &= V_B(h) + u(h)\quad ,\end{aligned}\tag{2}$$

where w, u, and θ are conveniently modeled as independent, nonstationary, white, Gaussian processes with probability density function (*pdf*) given by:

$$\begin{aligned}w &= N(\overline{w}(h),\, \sigma_w^2)\\ \theta &= N(\overline{\theta}(h),\, \sigma_\theta^2)\\ u &= N(\overline{u}(h),\, \sigma_u^2)\quad ,\end{aligned}\tag{3}$$

where $\overline{(\ )}$ and $\sigma_{(\ )}^2$ represent respectively the mean and variance of a Gaussian process $N(\ )$. Note that the mean and variance are functions of the balloon's instantaneous height, h, which in turn is implicitly a function of time. From Figure 4 it can be shown that the instantaneous height of the balloon is related to the $x\,y\,z$ coordinates by the relation

$$h(x,\, y,\, z) = \mathrm{Re}\left\{\sqrt{\left(1+\frac{z}{\mathrm{Re}}\right)^2 + \left(\frac{x}{\mathrm{Re}}\right)^2 + \left(\frac{y}{\mathrm{Re}}\right)^2} - 1\right\}\quad , \tag{4}$$

where Re is the earth's radius. Defining a columnwise state vector $\mathbf{x} = [x,\, y,\, z]^T$, and a columnwise uncertainty wind parameter vector $\mathbf{a} = [w,\, u,\, \theta]^T$, Equations (2), (3), and (4) can be combined to yield a state equation of the form

$$\dot{\mathbf{x}}(t) = \mathbf{f}(\mathbf{x}(t),\, \mathbf{a}(t),\, t)\quad , \tag{5}$$

where $\mathbf{f}(\ )$ is a vector function, and the wind parameter vector is a function of the state $\mathbf{x}$ through Equation (4). Thus the mathematical problem is to solve the stochastic vector differential Equation (5) with initial condition $\mathbf{x}(0) = \mathbf{x}_0$ (assume known) and the p.d.f. of $\mathbf{a}$ is given by:

$$\mathbf{a} = N\left(m\left(\mathbf{a}\right)\ ,\ \mathrm{cov}\left(\mathbf{a}\right)\right) \quad , \tag{6}$$

where the mean and covariance of $\mathbf{a}$ are given by

$$m(\mathbf{a}) = [\overline{w}(h), \overline{u}(h), \theta(h)]^T \quad , \tag{7}$$

$$\mathrm{cov}(\mathbf{a}) = \begin{bmatrix} \sigma_w^2(h) & 0 & 0 \\ 0 & \sigma_u^2(h) & 0 \\ 0 & 0 & \sigma_\theta^2(h) \end{bmatrix} \quad . \tag{8}$$

Equation (5) is difficult to solve in general* because (1) it is highly nonlinear and coupled *via* Equation (4), and (2) uncertainty parameters are functions of the state.

To a first-order approximation, the following assumptions can be made, which simplify the structure of Equation (5) significantly and subsequently yield a simple prediction algorithm.

The first assumption is that the horizontal flight range of the balloon from the launch point is small compared to the earth's radius, thus we have

$$\frac{x}{\mathrm{Re}} \ll 1 \quad , \tag{9}$$

$$\frac{y}{\mathrm{Re}} \ll 1 \quad . \tag{10}$$

So Equation (4) can be written as

$$h(z) \cong z \quad . \tag{11}$$

---

* *Applied Optimal Estimation*, M.I.T. Press, chapter 6.

The second assumption is that the vertical component of the wind velocity $u(h)$ is negligible compared to V_B, the balloon ascent speed. The third assumption is that the balloon ascent speed to a first-order is essentially independent of altitudes. Using the above three assumptions, the balloon's flight Equation (2) becomes

$$\dot{x}(t) = w(z) \quad \cos\theta(z) \quad , \tag{12}$$

$$\dot{y}(t) = w(z) \quad \sin\theta(z) \quad , \tag{13}$$

$$\dot{z}(t) = V_B \quad . \tag{14}$$

Now Equation (14) is decoupled from Equations (12) and (13) and that we have removed the state dependency of the uncertain wind parameter by integrating the $z(t)$ equation independently. Note that the $x(t)$ and $y(t)$ components are still coupled through the wind parameters. Since $z(t)$ is no longer a random parameter, we seek the mean and covariance propagation of the $x(t)$ and $y(t)$ components.

2. Computation of Balloon's Mean Trajectory

Integrating Equations (12) to (14) yield

$$x(t) = \int_0^t w(z)\cos\theta(z)\,d\tau \quad , \tag{15}$$

$$y(t) = \int_0^t w(z)\sin\theta(z)\,d\tau \quad , \tag{16}$$

$$z(t) = \int_0^t V_B\,d\tau \quad , \tag{17}$$

where the only random components are the $x(t)$ and $y(t)$ due to the wind uncertainty parameters. The mean values of $x(t)$ and $y(t)$ are obtained by taking the expected value of Equations (15) and (16), and yields

$$\begin{aligned}\hat{x}(t) &= \int_0^t E\{w(z)\cos\theta(z)\}\,d\tau \\ &= \int_0^t E\{w(z)\}\;E\{\cos\theta(z)\}\,d\tau \\ &= \int_0^t \hat{w}(z)\cos\hat{\theta}(z)\,d\tau \quad ,\end{aligned} \tag{18}$$

since $w(z)$ and $\theta(z)$ are independent processes, and the relation

$$E\{\cos(z)\} = \cos\hat{\theta}(z) \quad , \tag{19}$$

is obtained from the first-order expansion of $\cos\theta(z)$ about the current value of $z(t)$. Similar manipulation of Equation (16) yields:

$$\hat{y}(t) = \int_0^t \hat{w}(z)\sin\hat{\theta}(z)\,d\tau \quad . \tag{20}$$

Thus the balloon's mean trajectory is obtained by integrating simultaneously Equations (17), (18), and (20) with a given initial condition of $x(0)$, $y(0)$, and $z(0)$.

3. Computation of Balloon's Position Uncertainty

It is desired to obtain balloon's position uncertainty due to the random wind fluctuation. This can be done by computing the covariance propagation of x and y components. Toward this goal, we define the state vectors:

$$\mathbf{x}(t) = \begin{bmatrix} x(t) \\ y(t) \end{bmatrix} \quad , \tag{21}$$

and the wind parameter vector

$$\mathbf{a} = \begin{bmatrix} w \\ \theta \end{bmatrix} \quad , \tag{22}$$

so Equation (15) and (16) can be expressed as

$$\mathbf{x}(t) = \int_0^t \mathbf{f}(\mathbf{a})\, d\tau \quad . \tag{23}$$

Now linearizing $\mathbf{x}(t)$ about $\hat{\mathbf{x}}(t)$, $\hat{w}$, and $\hat{\theta}$; *i.e.*, the mean trajectory yields:

$$\delta\mathbf{x}(t) = \int_0^t \left.\frac{\partial f}{\partial \mathbf{a}}\right|_{\mathbf{a}=\hat{\mathbf{a}}} \delta\mathbf{a}\, d\tau \tag{24}$$

where it is defined

$$\delta\mathbf{x}(t) = \mathbf{x}(t) - \hat{\mathbf{x}}(t) \quad , \tag{24}$$

$$\delta\mathbf{a} = \mathbf{a} - \hat{\mathbf{a}} \quad , \qquad 26)$$

and

$$\begin{aligned} \left.\frac{\partial f}{\partial \mathbf{a}}\right|_{\mathbf{a}=\hat{\mathbf{a}}} &= \begin{bmatrix} \cos\hat{\theta} & -\hat{w}\sin\hat{\theta} \\ \sin\hat{\theta} & \hat{w}\cos\hat{\theta} \end{bmatrix} \\ &\stackrel{\triangle}{=} \hat{F} \quad , \end{aligned} \tag{27}$$

where $\delta(\ )$ is the Dirac-delta function. Therefore the covariance of $\delta\mathbf{x}(t)$ is given by

$$
\begin{aligned}
P &\stackrel{\triangle}{=} \mathrm{cov}(\delta\mathbf{x}) \\
&\stackrel{\triangle}{=} E[\,\delta\mathbf{x} \quad \delta\mathbf{x}^T] \\
&= \begin{bmatrix} \sigma_x^2 & \sigma_{xy}^2 \\ \sigma_{xy}^2 & \sigma_y^2 \end{bmatrix} \\
&= \int_0^t \int_0^t \hat{F} Q(\tau_1, \tau_2) \hat{F}^T \, d\tau_1 \, d\tau_2 \quad ,
\end{aligned}
\tag{28}
$$

where we have defined

$$
\begin{aligned}
Q(\tau_1, \tau_2) &= E\{\delta\mathbf{a}(\tau_1)\, \delta\mathbf{a}^T(\tau_2)\} \\
&= \begin{bmatrix} \sigma_w^{*2}\, \delta(\tau_1 - \tau_2) & 0 \\ 0 & \sigma_\theta^2\, \delta(\tau_1 - \tau_2) \end{bmatrix} \quad .
\end{aligned}
\tag{29}
$$

Now substituting $\hat{F}$ in Equation (27) and Q in Equation (29) into (28) and simplifying yields the desired expressions for the covariance propagation uncertainty:

$$
\sigma_x^2 = \int_0^t \left[(\cos\,\hat{\theta})^2\, \sigma_w^2 + (\hat{w}\,\sin\,\hat{\theta})^2\, \sigma_\theta^2 \right] d\tau \quad , \tag{30}
$$

$$
\sigma_y^2 = \int_0^t \left[(\sin\,\hat{\theta})^2\, \sigma_w^2 + (\hat{w}\,\cos\,\hat{\theta})^2\, \sigma_\theta^2 \right] d\tau \tag{30}
$$

and

$$
\sigma_{xy}^2 = \int_0^t \left[(\sin\,\hat{\theta}\ \cos\,\hat{\theta})\sigma_w^2 - (\hat{w}\,\sin\,\hat{\theta}\ \cos\,\hat{\theta})\sigma_\theta^2 \right] d\tau \quad . \tag{32}
$$

4. Computation of Balloon's CEP

Given a balloon's uncertainty covariance, one can compute its CEP, or circular error probability. CEP is the radius of the circle where there exists a 50% probability that the balloon is within the circle. Given a covariance matrix P, one could compute its eigenvalues from computing the determinant of $P - \lambda I$, or

$$\text{Det}\,|P - \lambda I| = 0 \quad . \tag{33}$$

In this case it resulted in a quadratic equation

$$\lambda^2 - (\sigma_x^2 + \sigma_y^2)\lambda + \sigma_x^2\sigma_y^2 - \sigma_{xy}^4 = 0 \quad , \tag{34}$$

which yields eigenvalues

$$\lambda_1 = \frac{b}{2} + \frac{\sqrt{b^2 - 4c}}{2} \quad , \tag{35}$$

$$\lambda_2 = \frac{b}{2} - \frac{\sqrt{b^2 - 4c}}{2} \quad , \tag{36}$$

where

$$b = \sigma_x^2 + \sigma_y^2 \quad , \tag{37}$$

$$c = \sigma_x^2\sigma_y^2 - \sigma_{xy}^4 \quad . \tag{38}$$

It can be shown* that CEP is related to the eigenvalues through the equation

$$\text{CEP} = .59\left(\sqrt{\lambda_1} + \sqrt{\lambda_2}\right) \quad . \tag{39}$$

* James Constant, "Fundamentals of Strategic Weapons Offense and Defense Systems," Martinus Nijhoff Publisher, 1981, pp. 201.

5. Description of Results

The predicted mean and covariance of the balloon's flight path were computed using Equations (15) to (17), and (30) to (32) respectively. The CEP is also computed using Equations (35) to (39). For the wind velocity profile shown in Figure 2, the resulting CEP is given in Figure 5. Note that the wind speeds increase linearly as a function of altitudes and peaked at about 40,000 feet with a maximum speed of 60 knots. Above this altitude, wind speeds decrease linearly to zero.

Assuming a constant ascent rate of 800 feet/minute for the balloon, it will reach the maximum wind speed altitude in about 50 minutes. Note that the CEP curve shown in Figure 5 depicts similar characteristics, since CEP, in effect, is related to the integral of wind speed. During the second hour of flight, the balloon slows down substantially due to reduction in wind speed and buoyancy. The balloon reaches its maximum altitude of 80,000 feet in about two hours.

Figure 6 shows the balloon position projected on the earth surface for the wind velocity profile given in Figure 2. The solid curve is the mean trajectory. CEPs are superimposed on the mean trajectory at 10 minute intervals. It can be seen that at the end of a two-hour flight, the balloon's CEP could be as large as 5 nautical miles.

Weather data changes from month to month. For completeness a full set of predictions was generated for weather data gathered at or around San Nicholas Island, the planned location for the observation experiment. These data were included in Appendix A.

6. Summary and Conclusions

Based on simplified assumptions, a first-order prediction algorithm was developed to estimate the balloon flight path. The estimates were given in terms of the mean (the average location) and the CEP (the 50% probability circle) as a function of time. The prediction algorithm was implemented and used to generate predictions for weather data from San Nicholas Island from January to December.

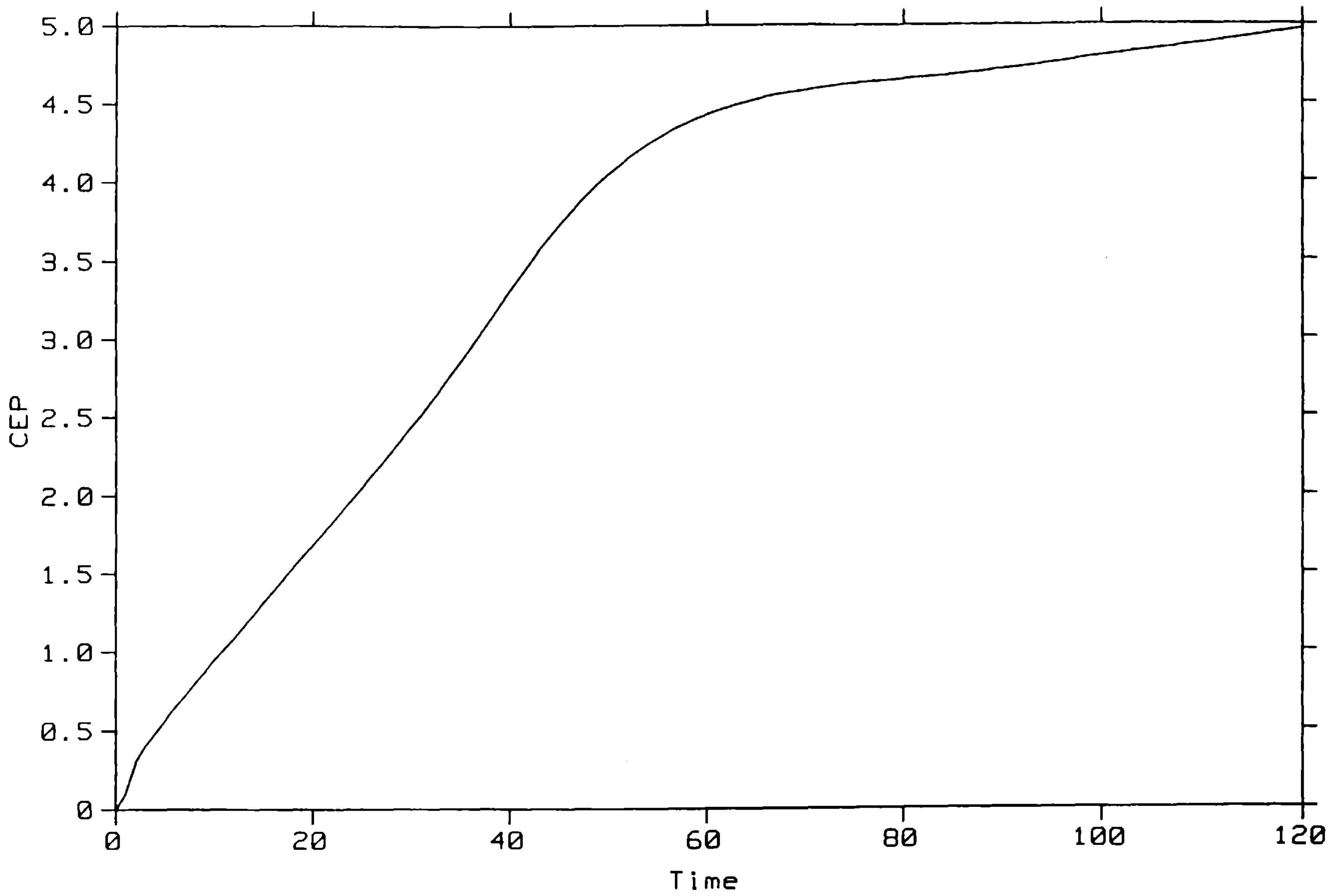

Figure 5. CEP (knots) vs. Time (min), weather data from San Nicholas Island typical for the month of February.

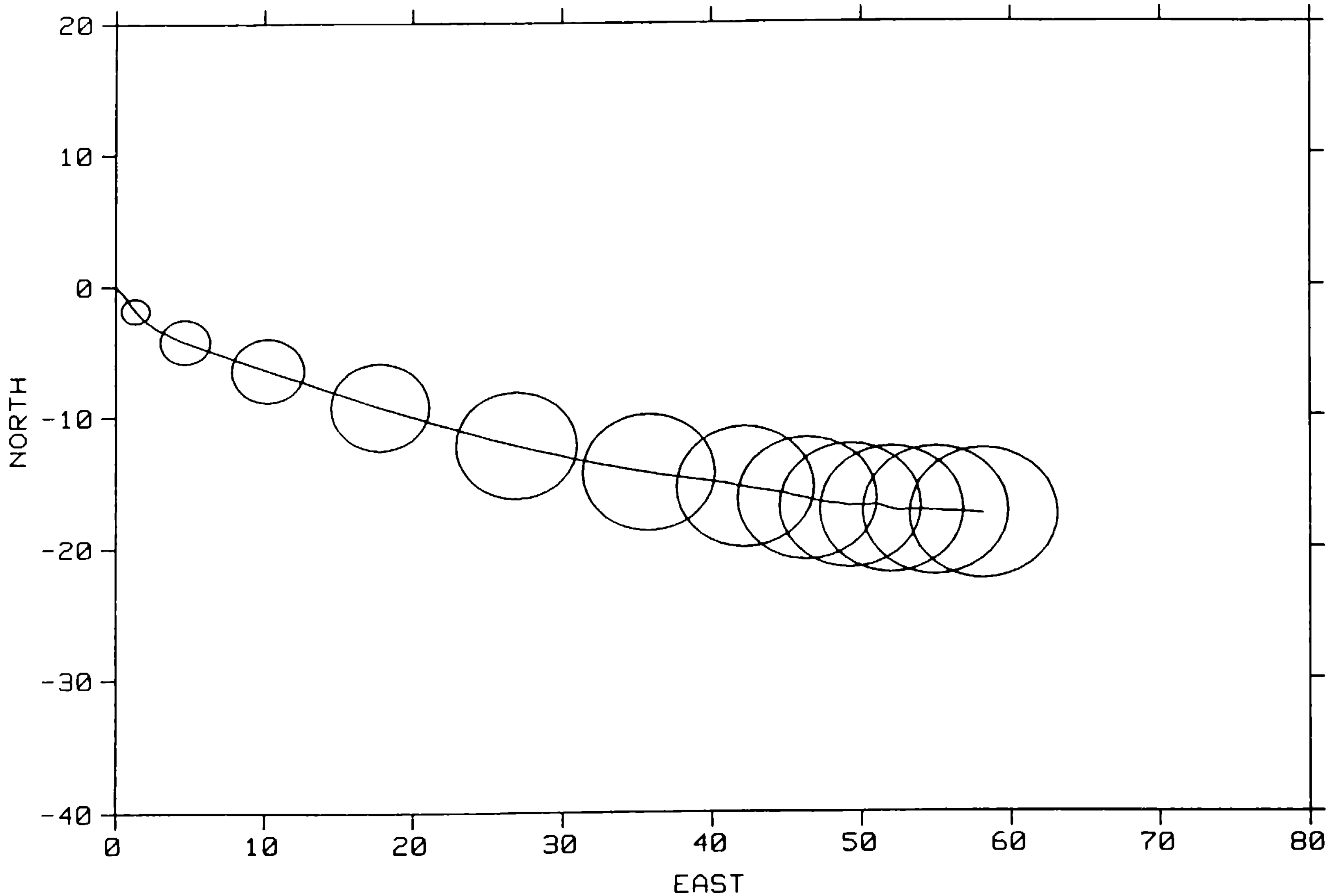

Figure 6. Balloon trajectory projected on earth surface showing CEP boundaries at 10 minute intervals. (units = knots) Weather data from San Nicholas Island typical for the month of February.

Appendix A

Balloon Position Prediction Near San Nicholas Island from January to December

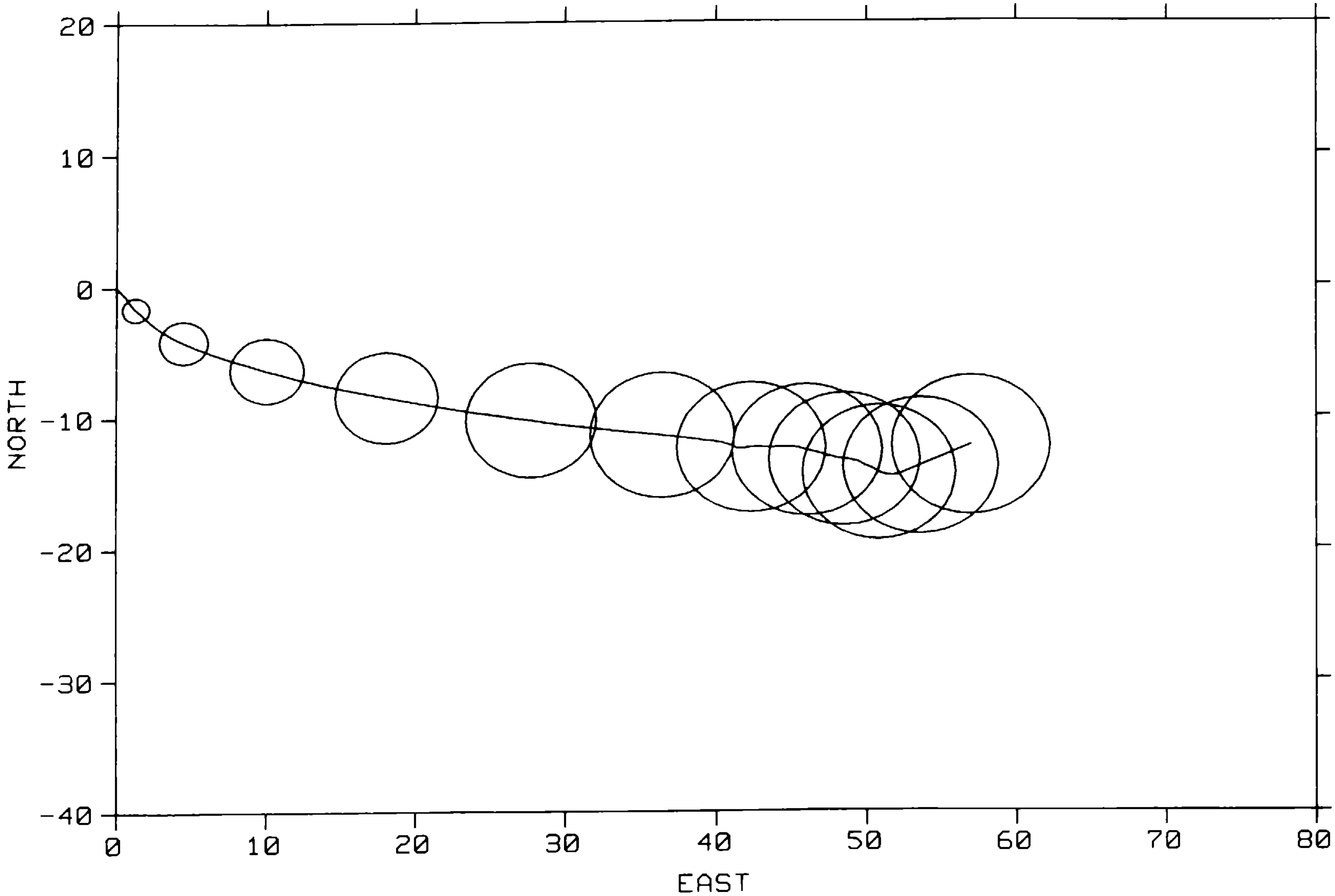

Figure 7. Balloon trajectory projected on earth surface showing CEP boundaries at 10 minute intervals. (units = knots) Weather data from San Nicholas Island typical for the month of January.

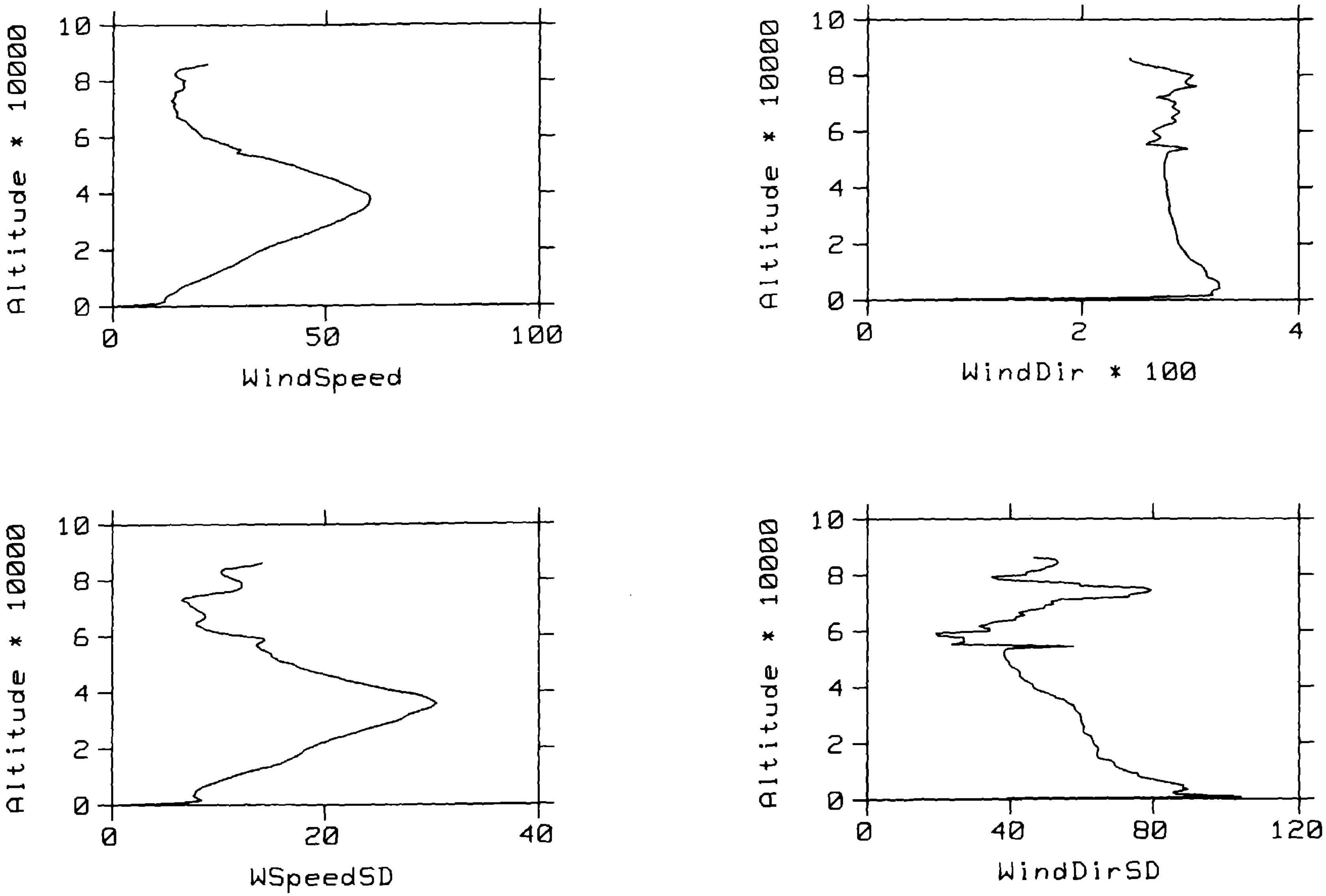

Figure 8. Altitude in feet, wind speed in knots, wind direction in degrees clockwise from North, weather data from San Nicholas Island typical for the month of January.

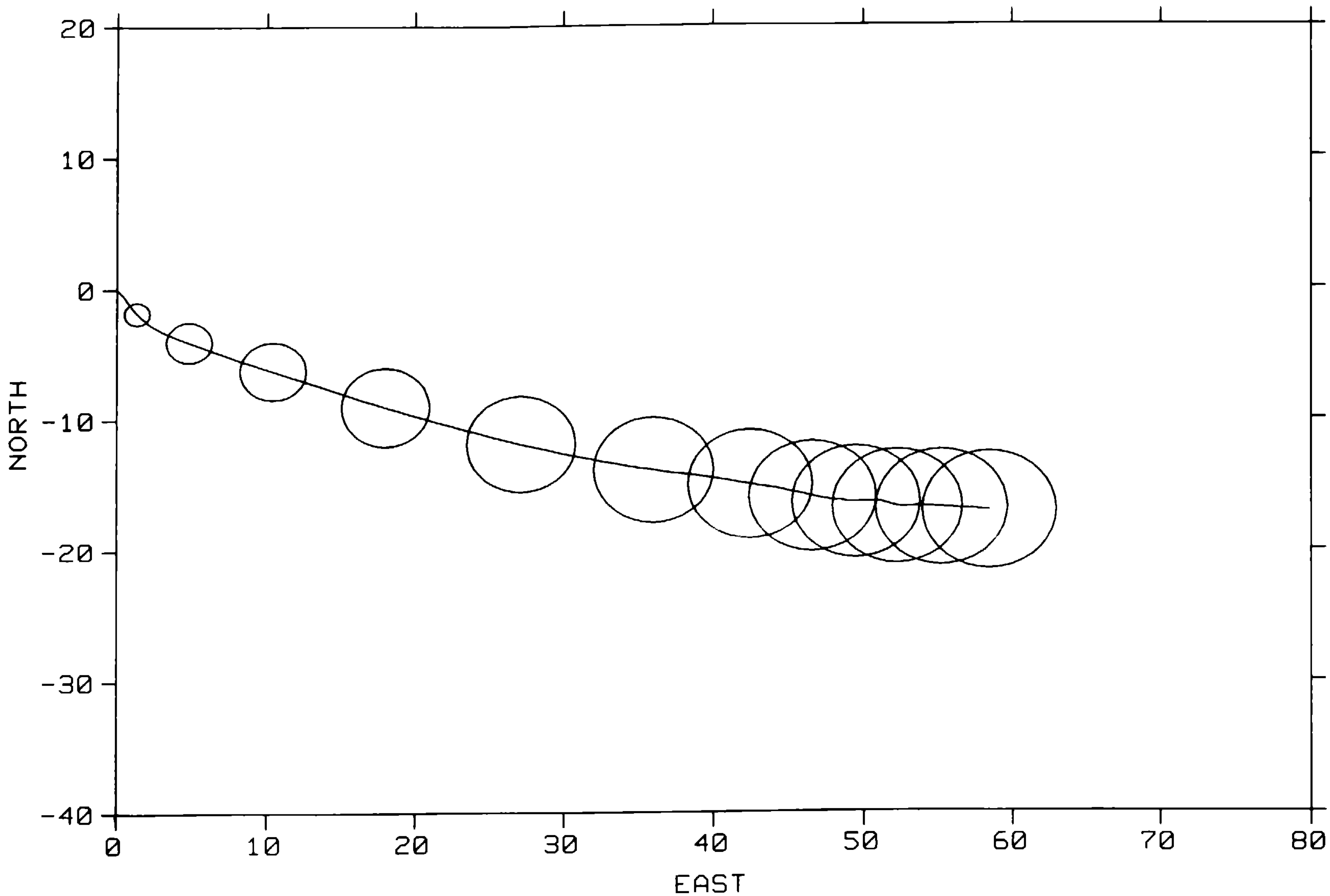

Figure 9. Balloon trajectory projected on earth surface showing CEP boundaries at 10 minute intervals. (units = knots) Weather data from San Nicholas Island typical for the month of February.

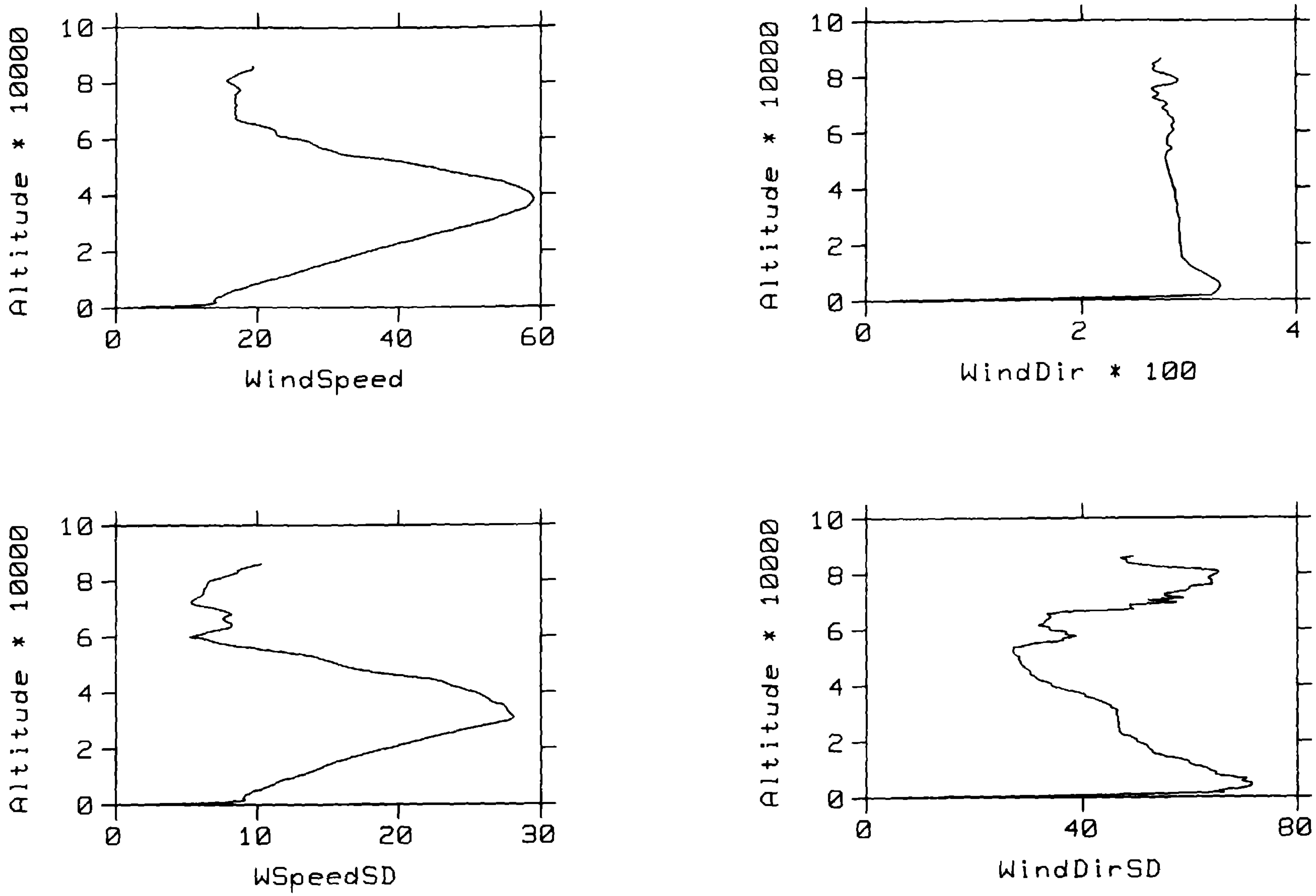

Figure 10. Altitude in feet, wind speed in knots, wind direction in degrees clockwise from North, weather data from San Nicholas Island typical for the month of February.

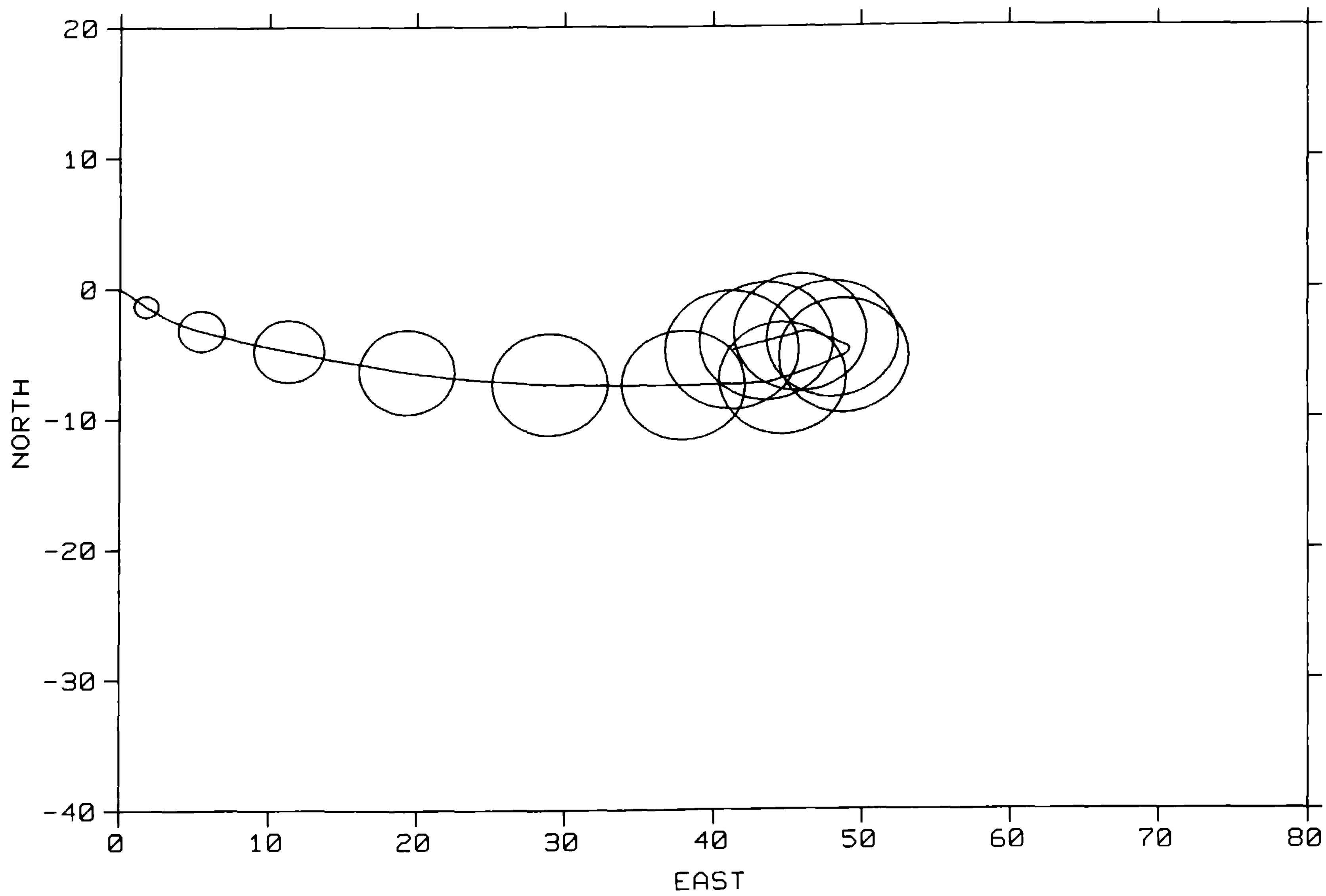

Figure 11. Balloon trajectory projected on earth surface showing CEP boundaries at 10 minute intervals. (units = knots) Weather data from San Nicholas Island typical for the month of March.

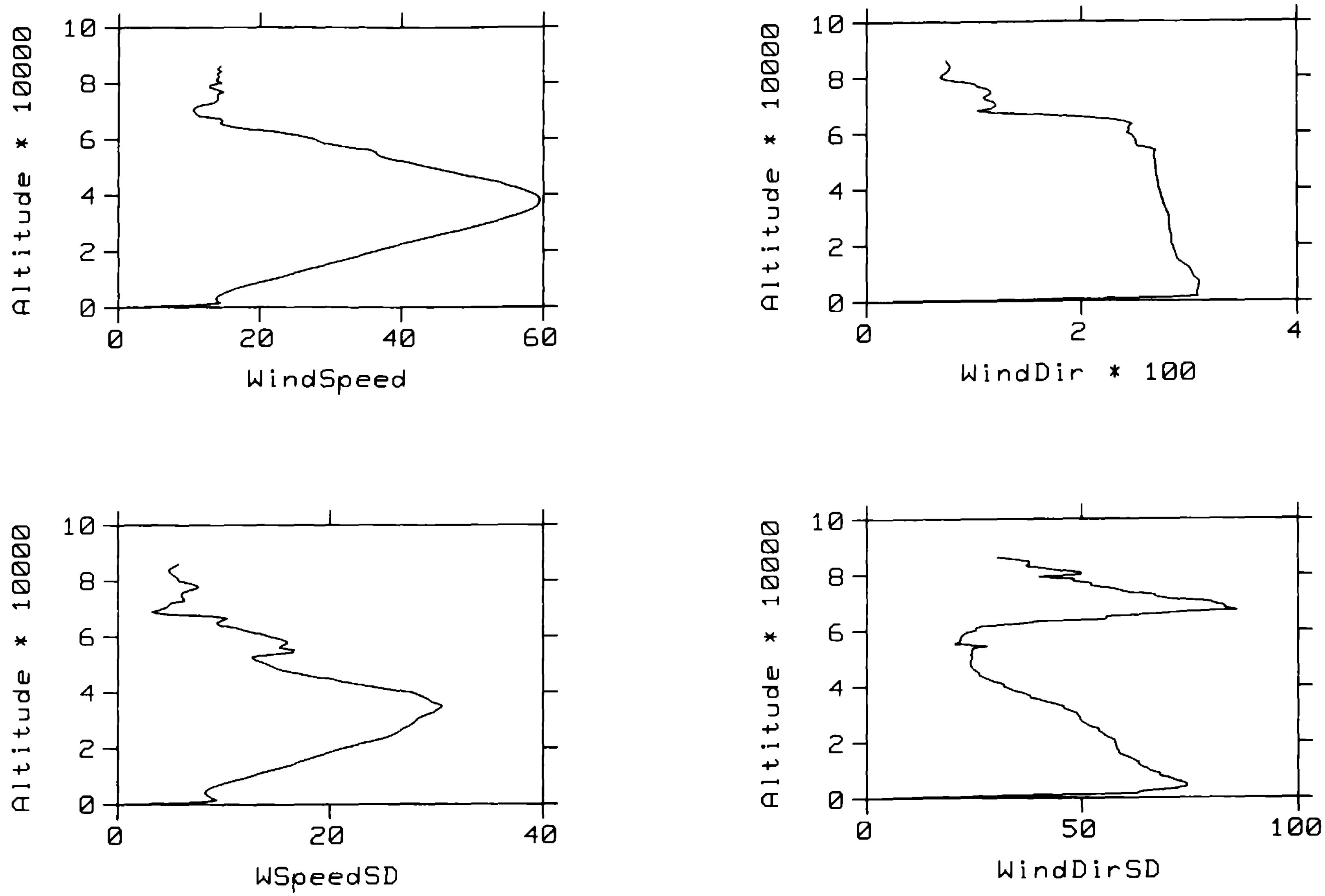

Figure 12. Altitude in feet, wind speed in knots, wind direction in degrees clockwise from North, weather data from San Nicholas Island typical for the month of March.

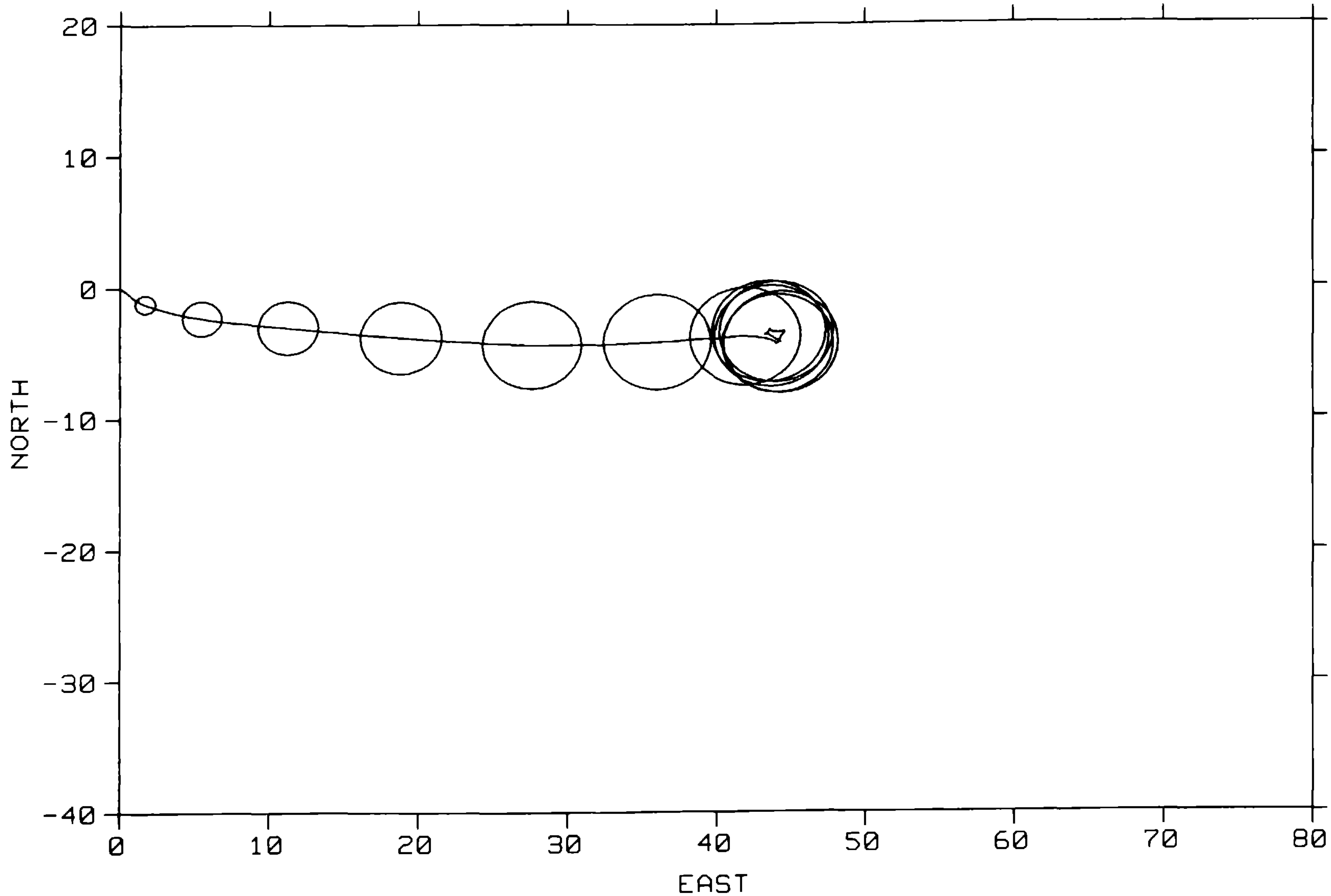

Figure 13. **Balloon trajectory projected on earth surface showing CEP boundaries at 10 minute intervals.** (units = knots) Weather data from San Nicholas Island typical for the month of April.

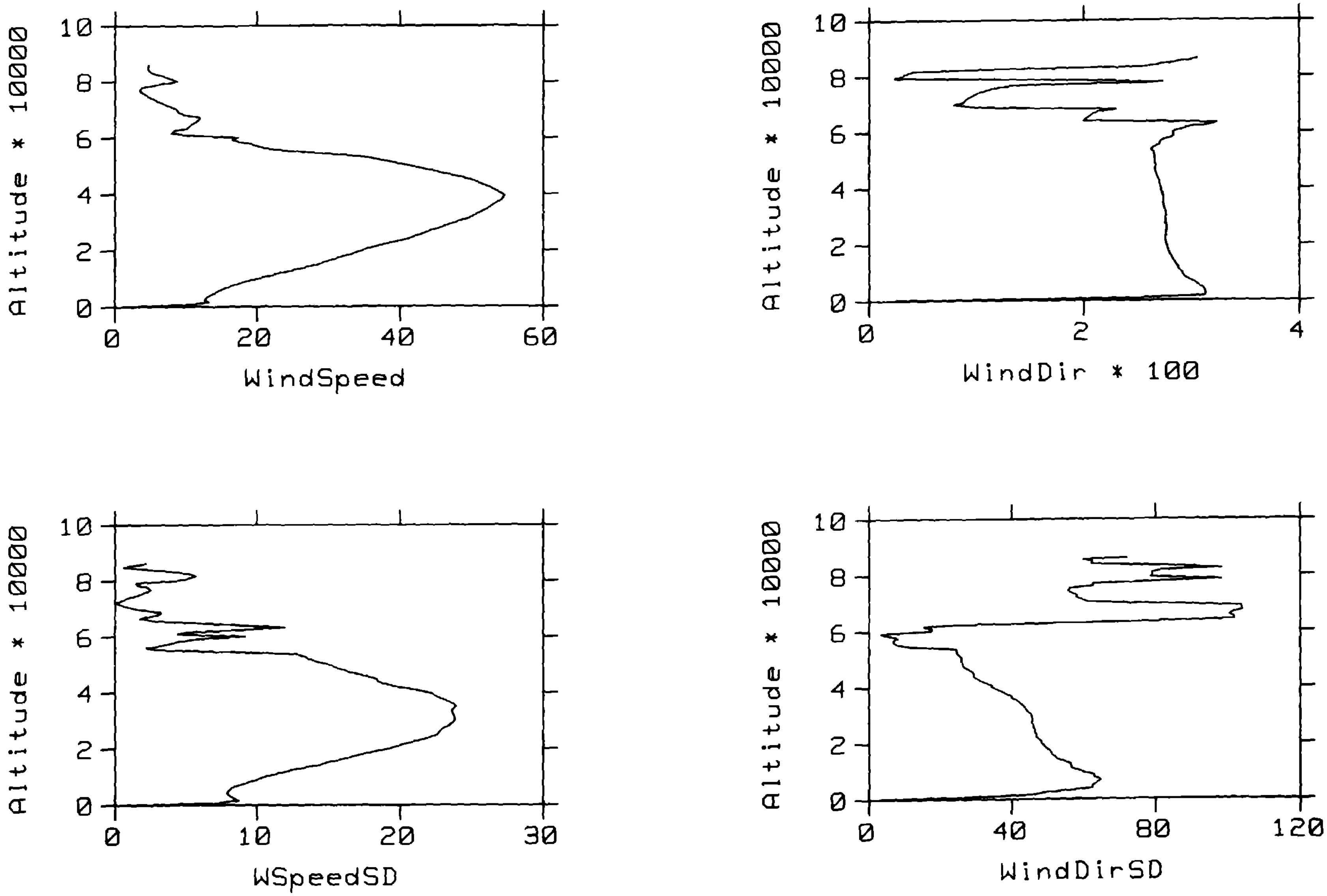

Figure 14. Altitude in feet, wind speed in knots, wind direction in degrees clockwise from North, weather data from San Nicholas Island typical for the month of April.

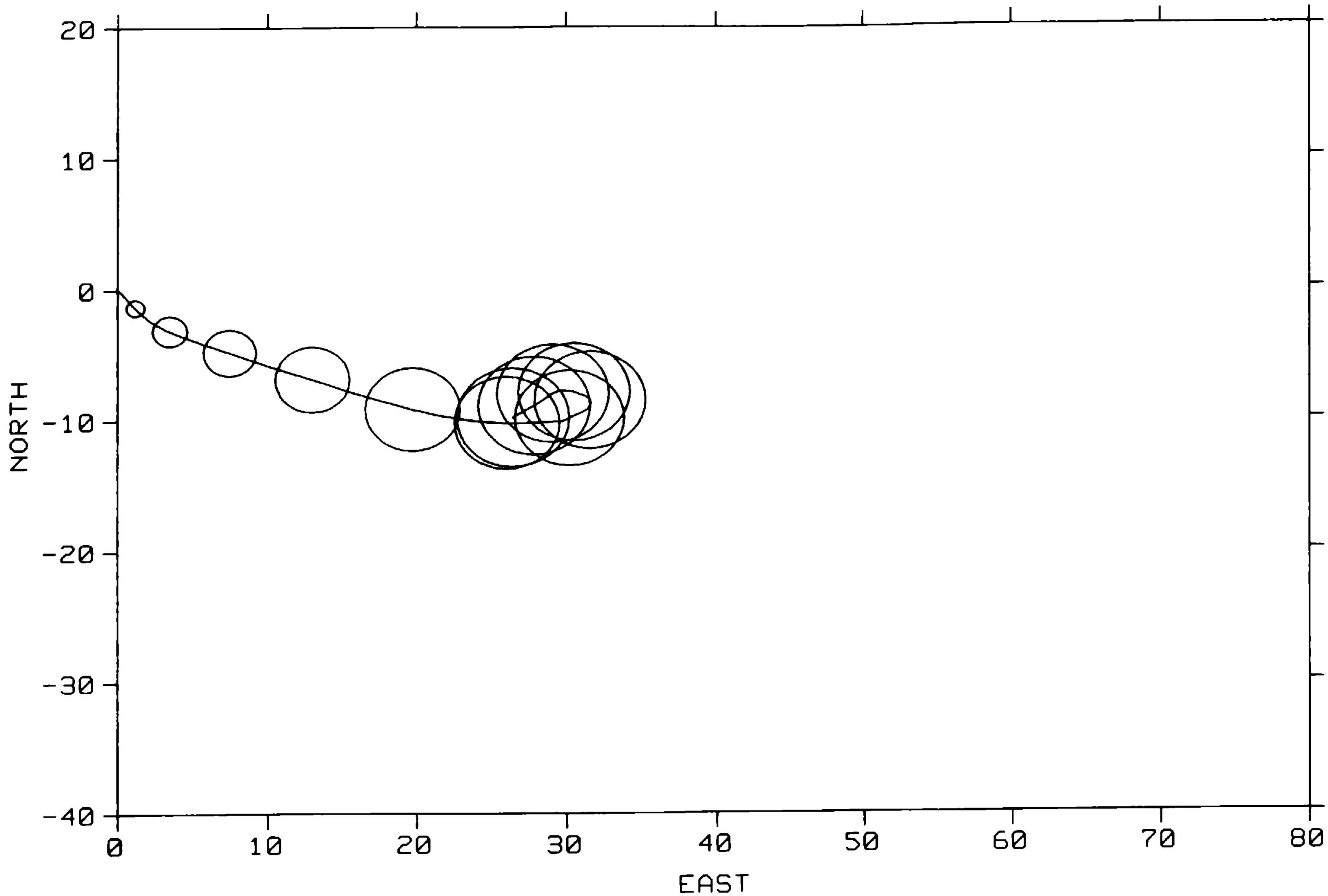

Figure 15. Balloon trajectory projected on earth surface showing CEP boundaries at 10 minute intervals. (units = knots) Weather data from San Nicholas Island typical for the month of May.

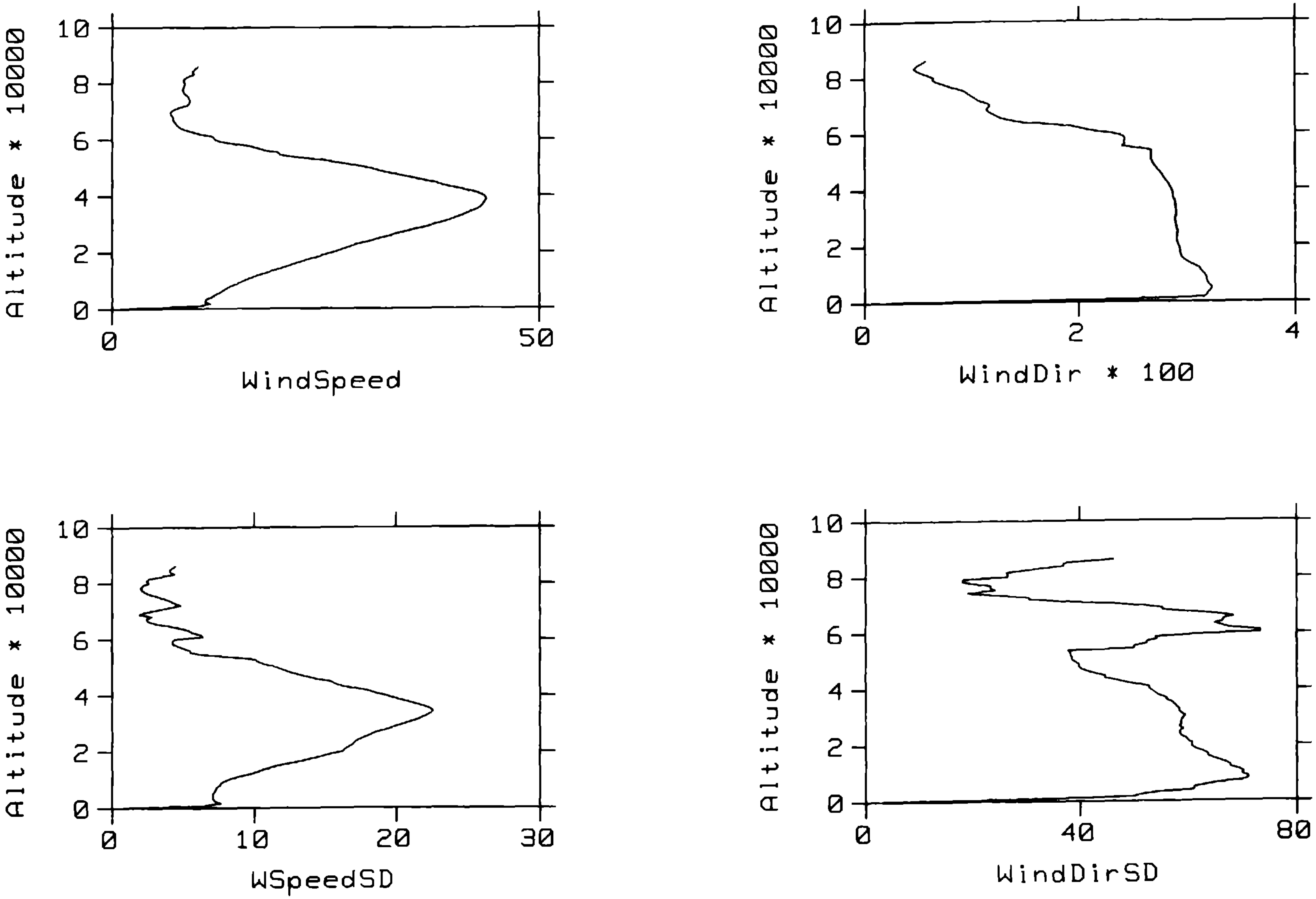

Figure 16. Altitude in feet, wind speed in knots, wind direction in degrees clockwise from North, weather data from San Nicholas Island typical for the month of May.

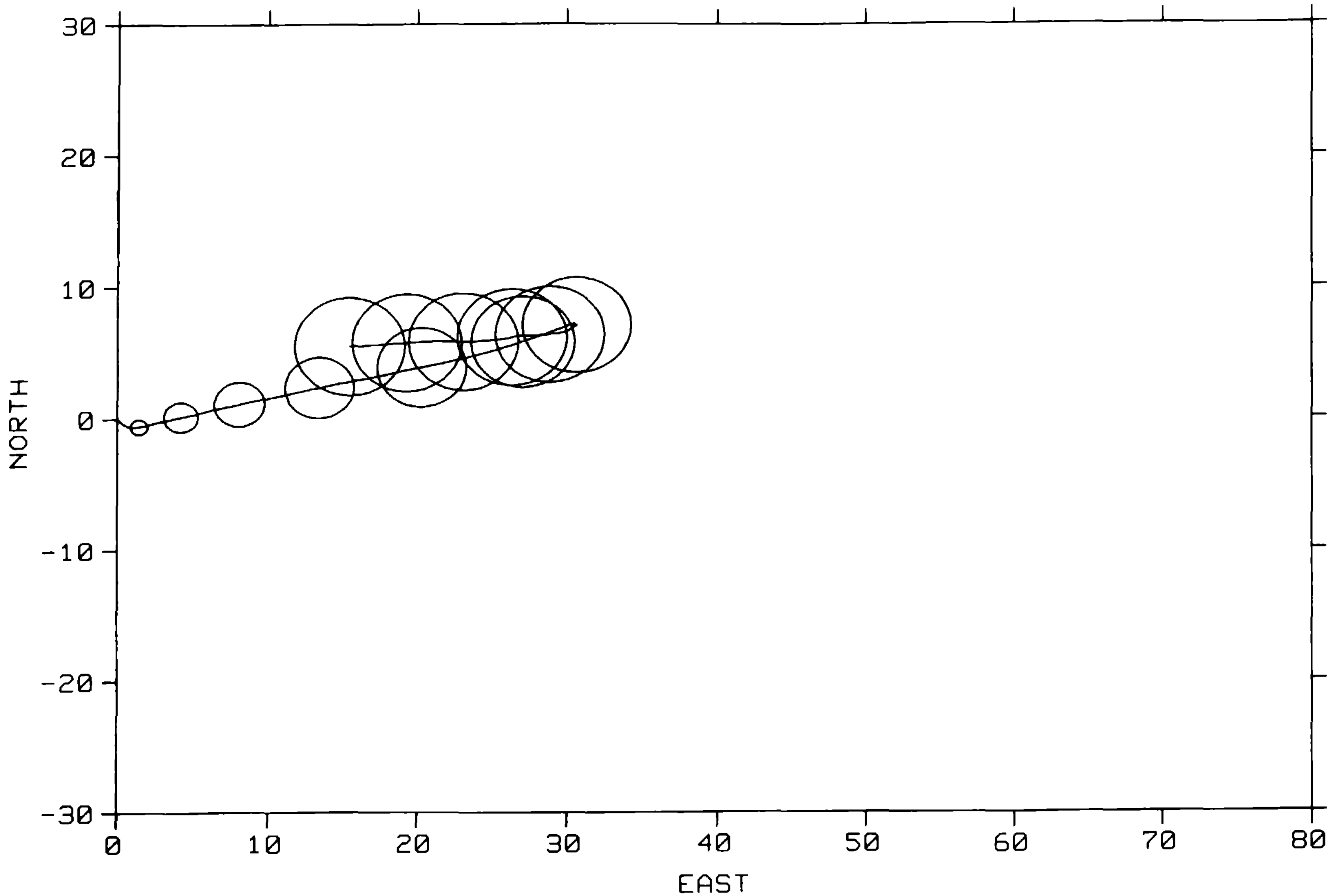

Figure 17. **Balloon trajectory projected on earth surface showing CEP boundaries at 10 minute intervals.** (units = knots) Weather data from San Nicholas Island typical for the month of June.

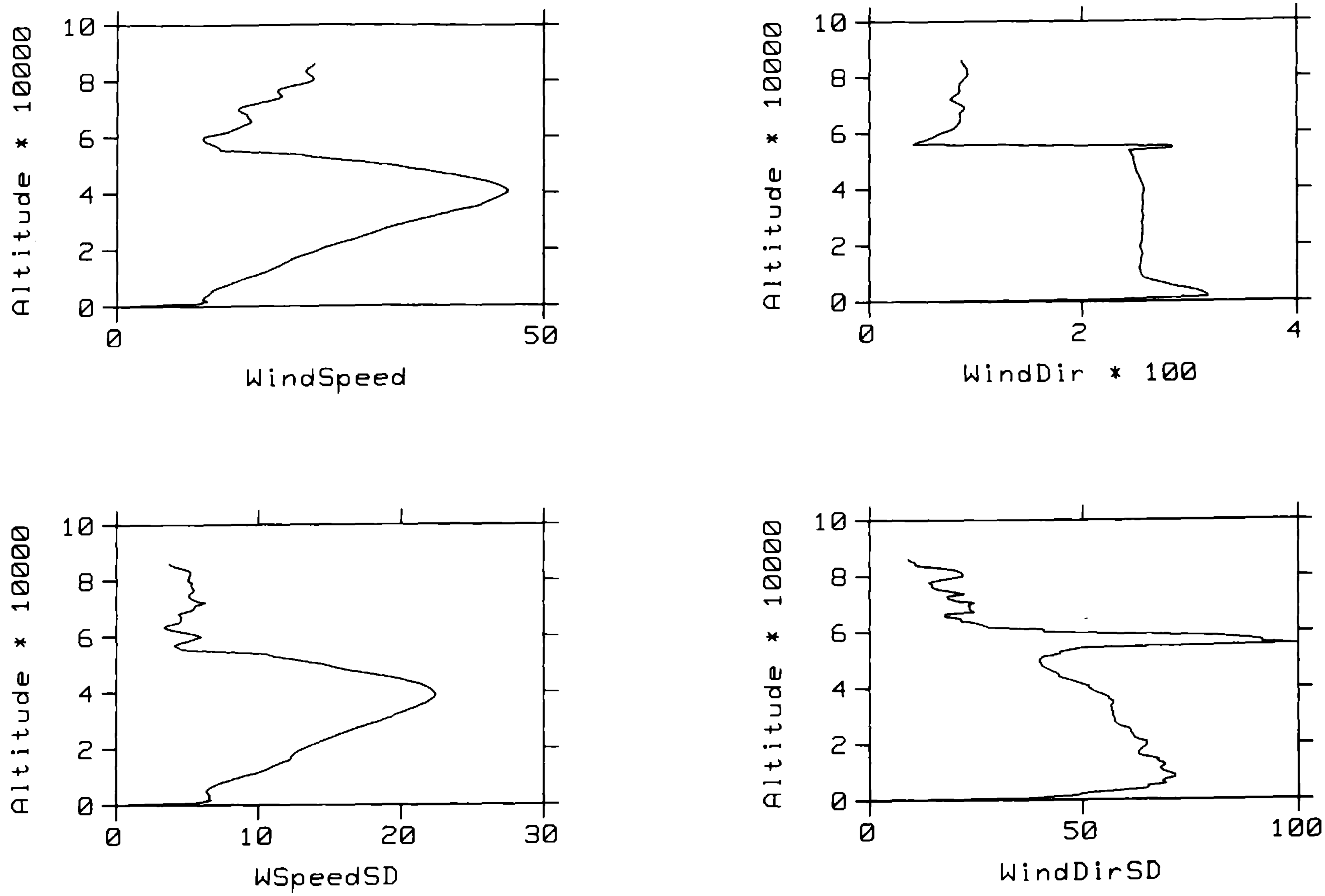

Figure 18. Altitude in feet, wind speed in knots, wind direction in degrees clockwise from North, weather data from San Nicholas Island typical for the month of June.

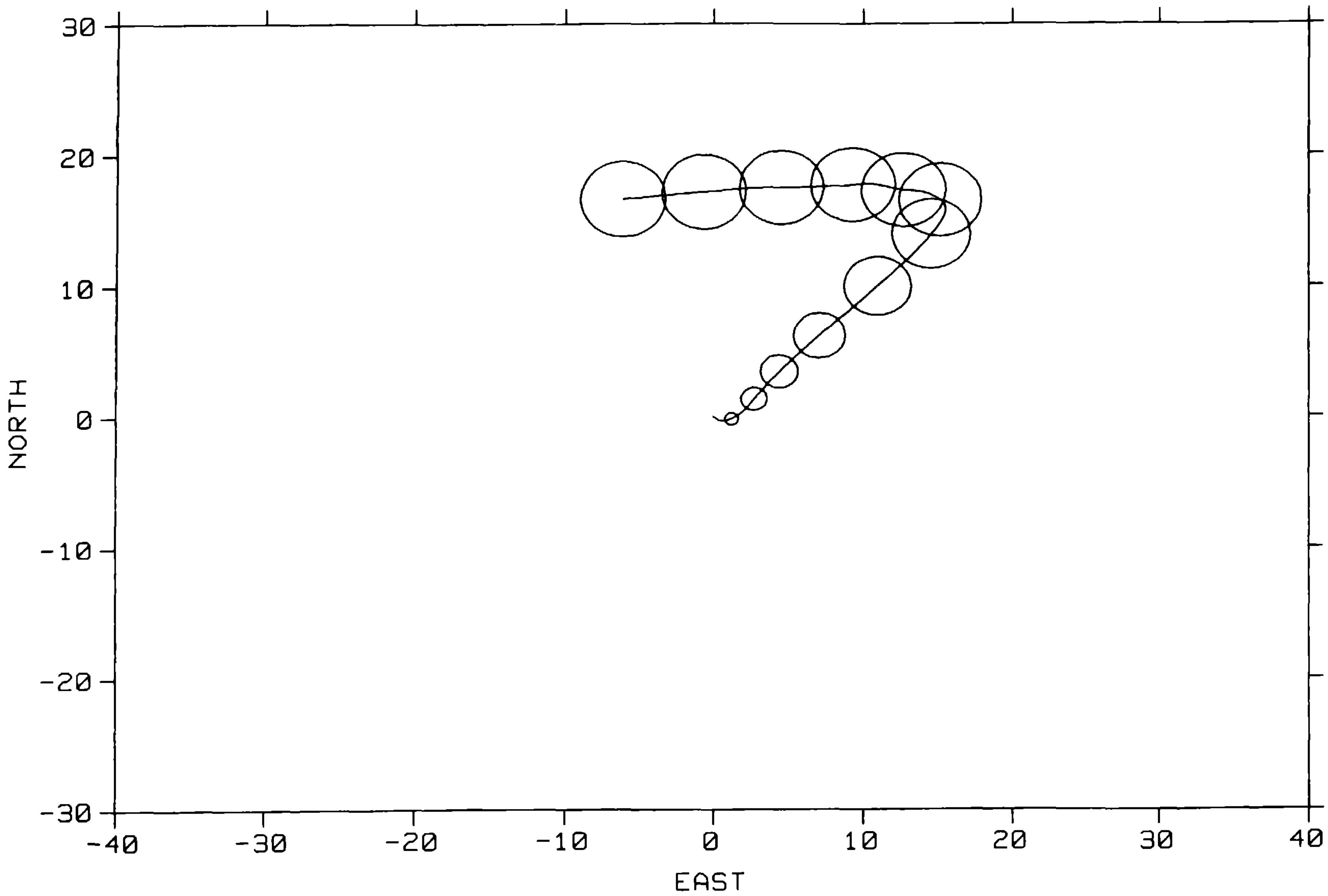

Figure 19. Balloon trajectory projected on earth surface showing CEP boundaries at 10 minute intervals. (units = knots) Weather data from San Nicholas Island typical for the month of July.

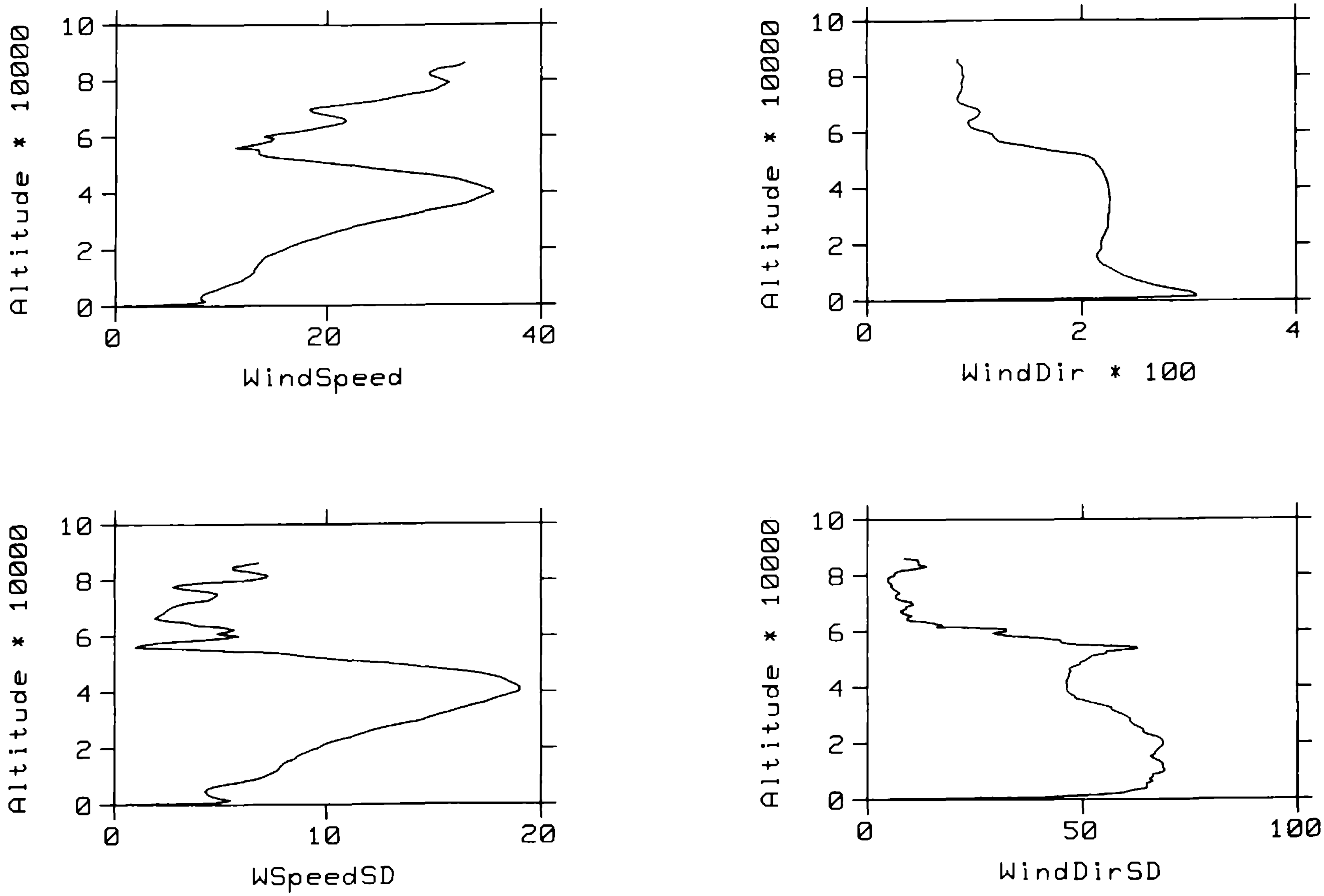

Figure 20. Altitude in feet, wind speed in knots, wind direction in degrees clockwise from North, weather data from San Nicholas Island typical for the month of July.

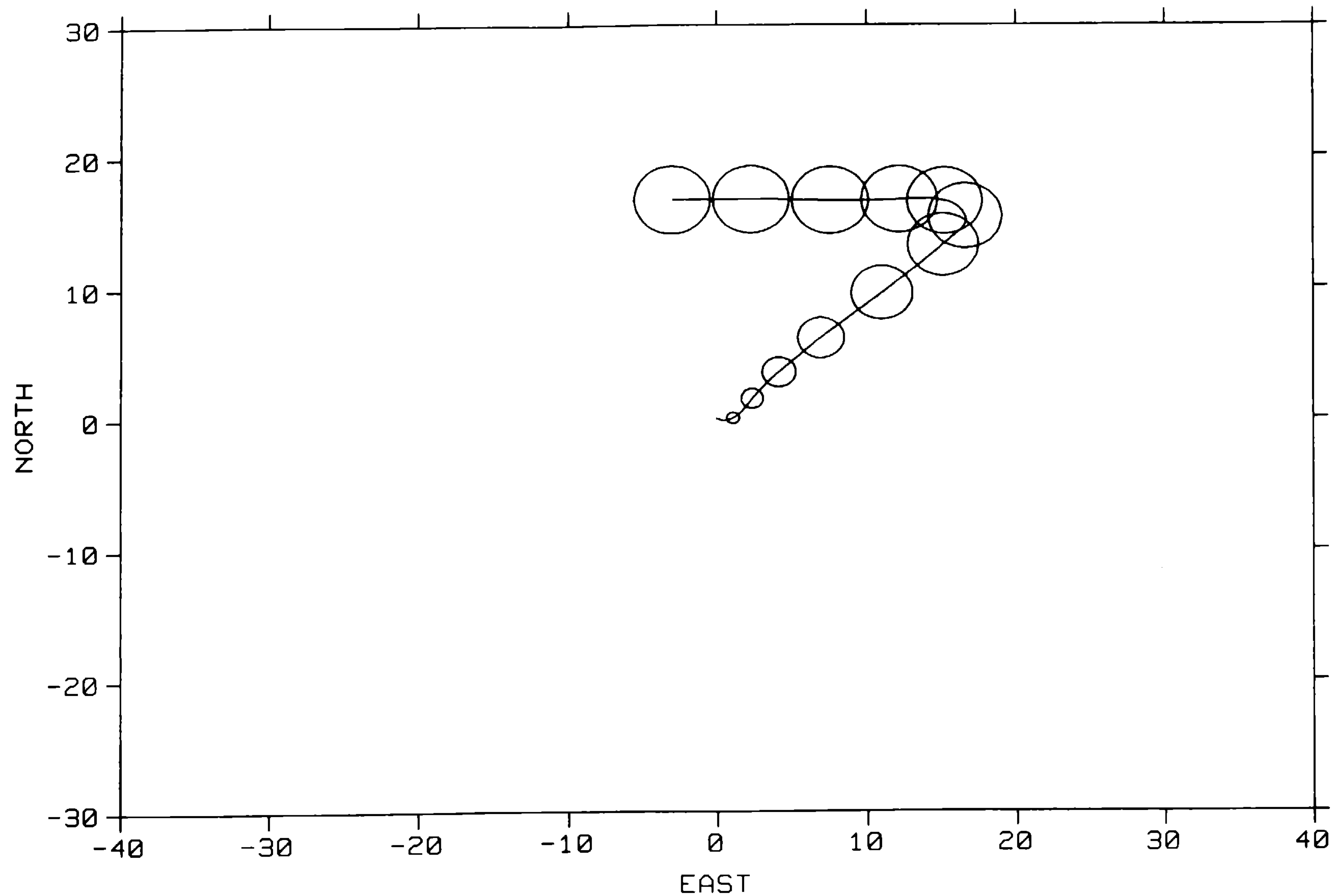

Figure 21. **Balloon trajectory projected on earth surface showing CEP boundaries at 10 minute intervals.** (units = knots) Weather data from San Nicholas Island typical for the month of August.

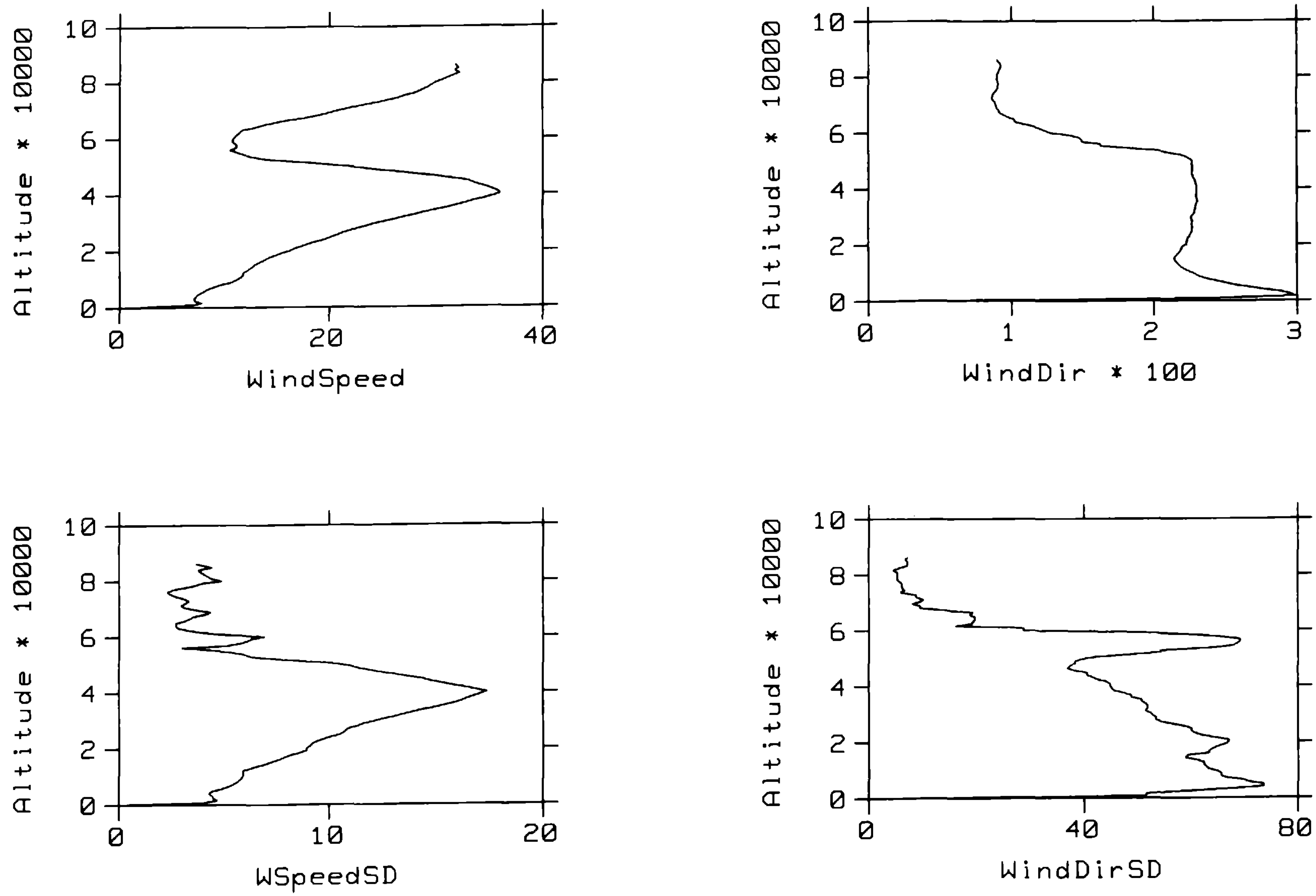

Figure 22. Altitude in feet, wind speed in knots, wind direction in degrees clockwise from North, weather data from San Nicholas Island typical for the month of August.

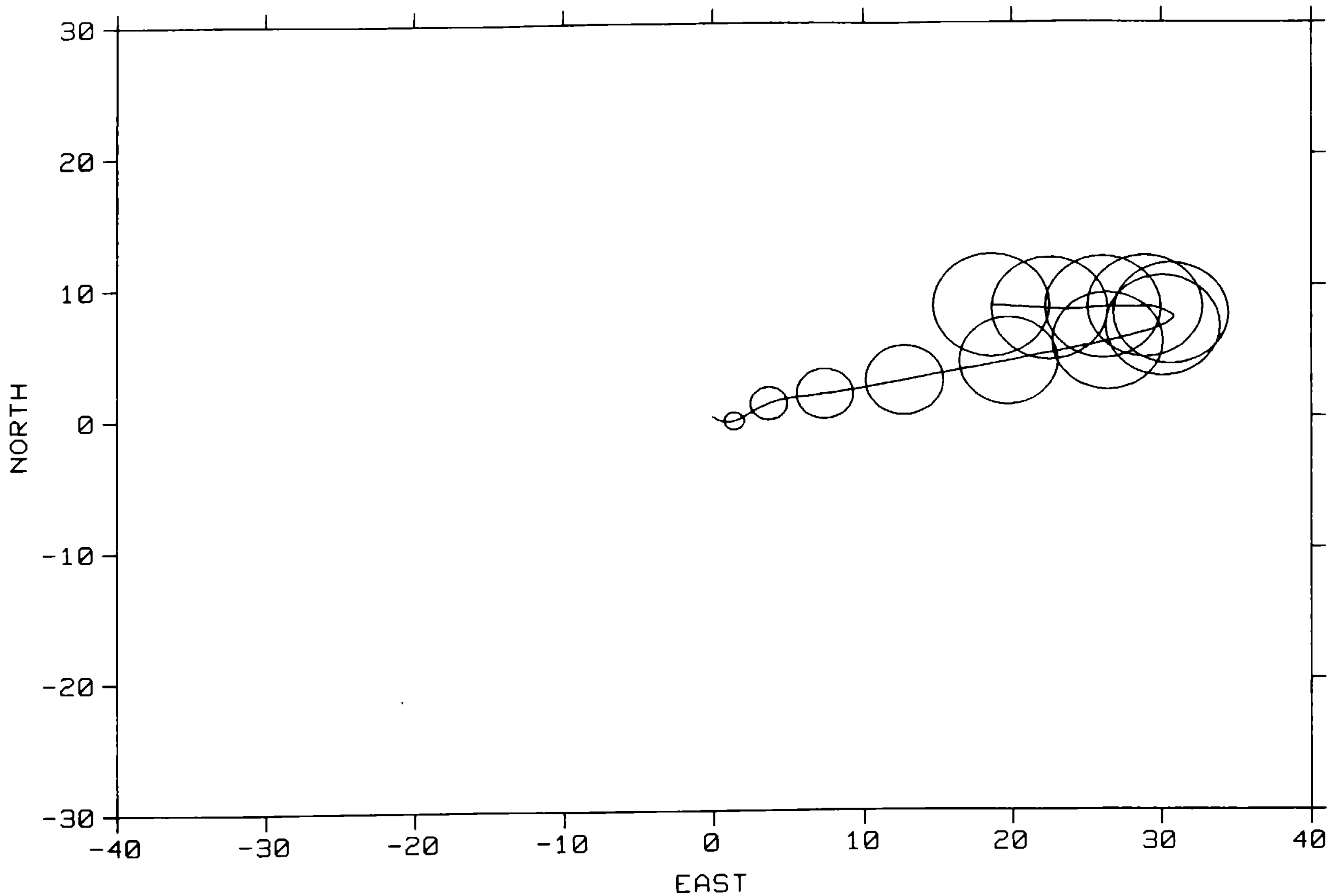

Figure 23. Balloon trajectory projected on earth surface showing CEP boundaries at 10 minute intervals. (units = knots) Weather data from San Nicholas Island typical for the month of September.

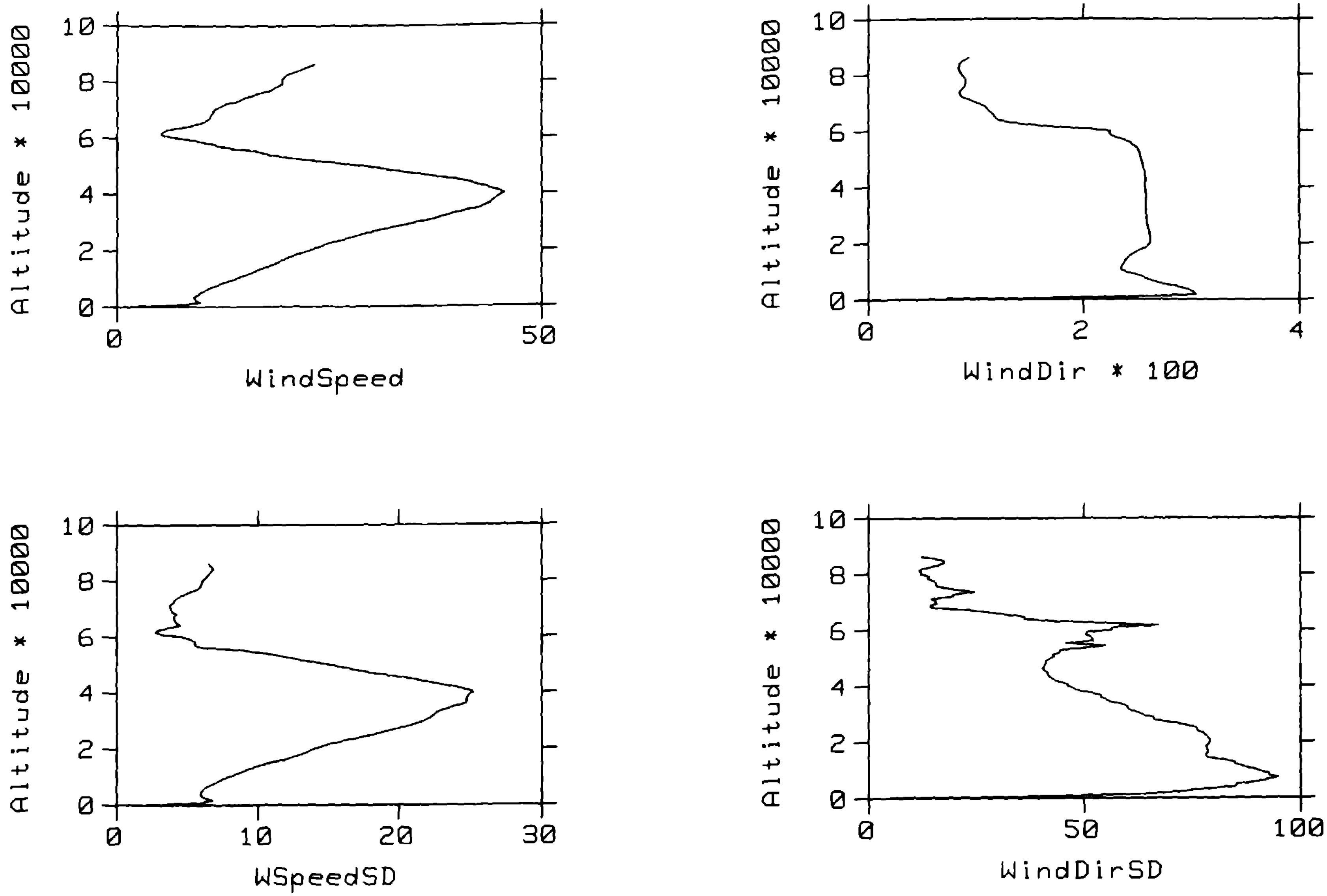

Figure 24. Altitude in feet, wind speed in knots, wind direction in degrees clockwise from North, weather data from San Nicholas Island typical for the month of September.

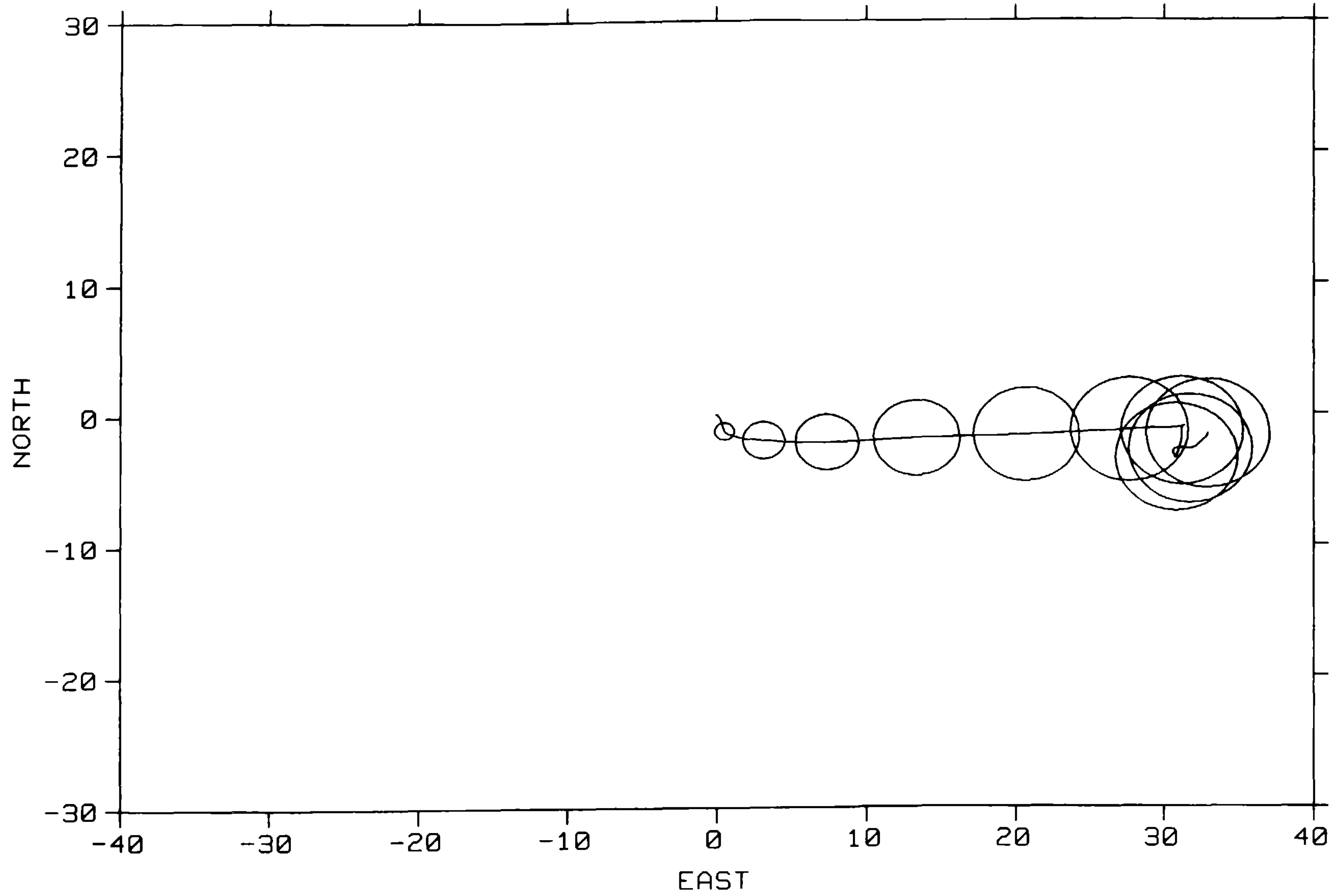

Figure 25. Balloon trajectory projected on earth surface showing CEP boundaries at 10 minute intervals. (units = knots) Weather data from San Nicholas Island typical for the month of October.

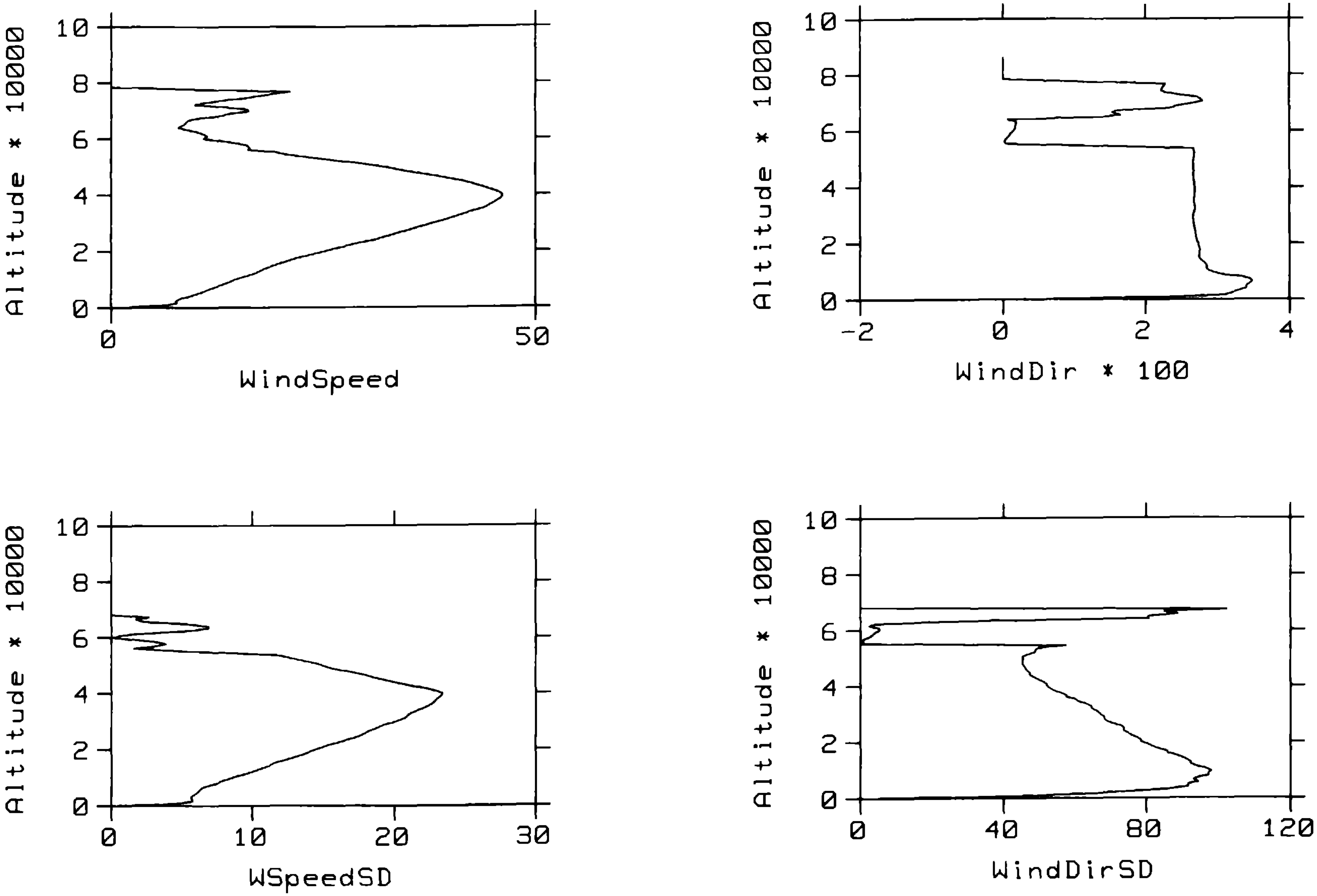

Figure 26. Altitude in feet, wind speed in knots, wind direction in degrees clockwise from North, weather data from San Nicholas Island typical for the month of October.

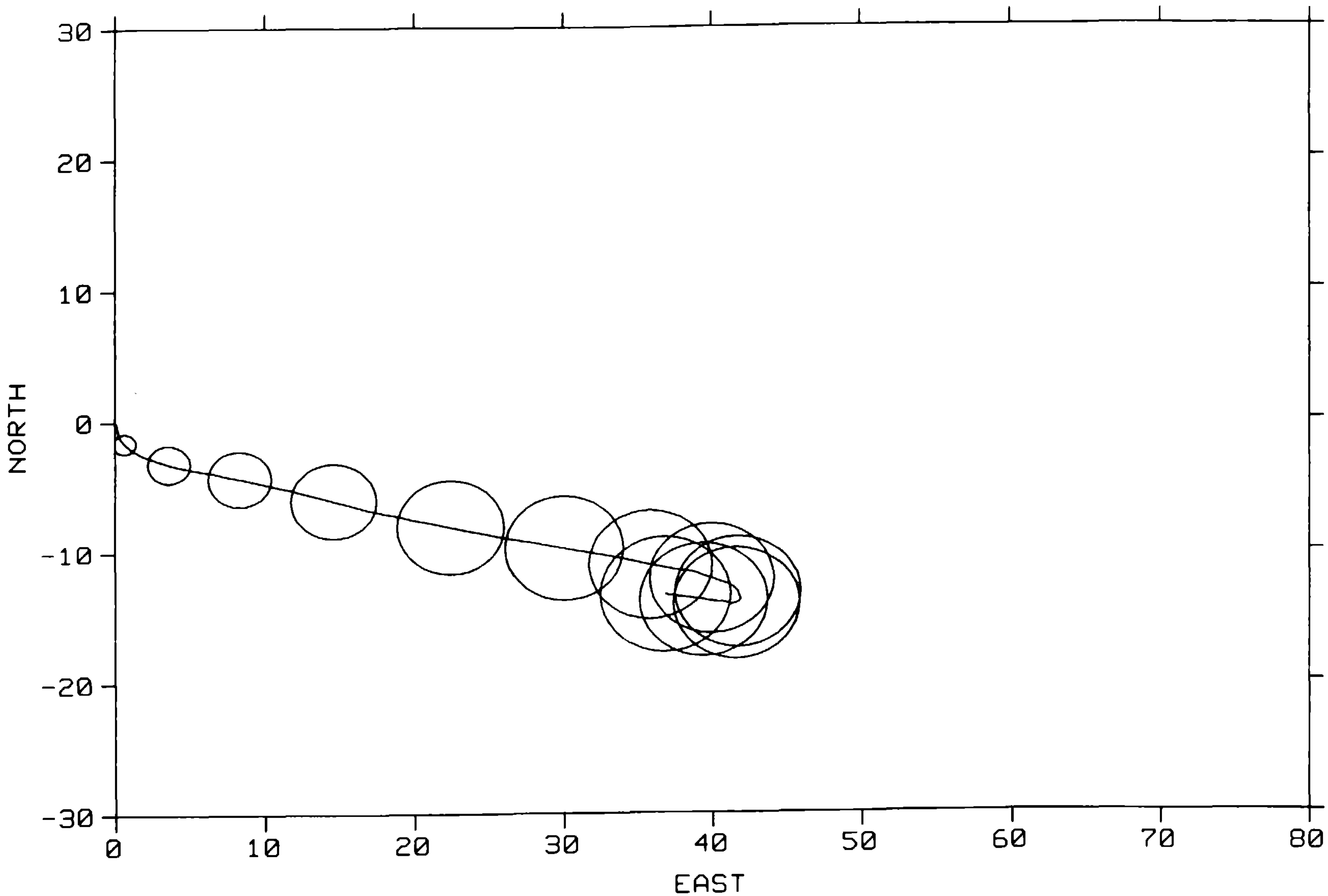

Figure 27. **Balloon trajectory projected on earth surface showing CEP boundaries at 10 minute intervals.** (units = knots) Weather data from San Nicholas Island typical for the month of November.

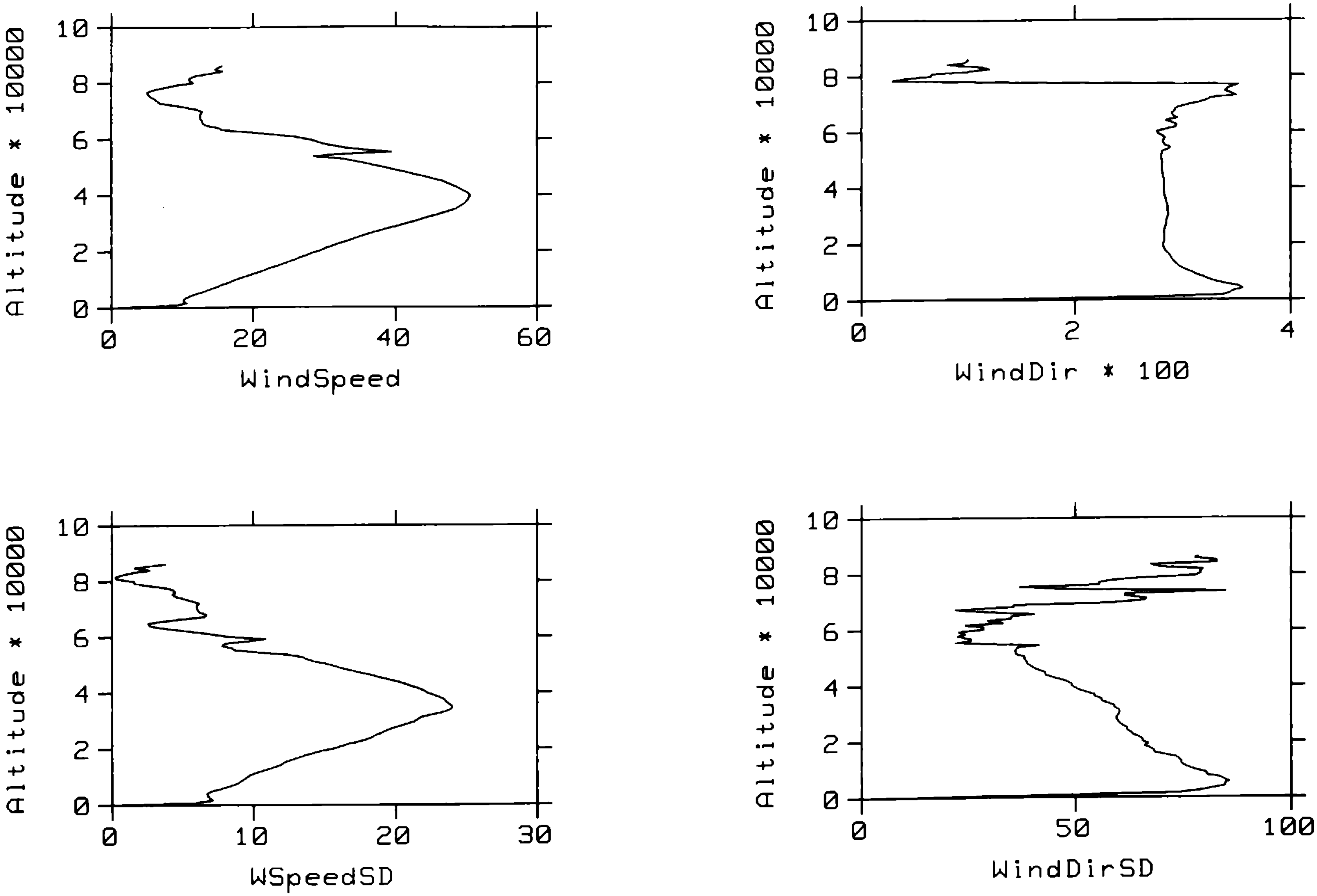

Figure 28. Altitude in feet, wind speed in knots, wind direction in degrees clockwise from North, weather data from San Nicholas Island typical for the month of November.

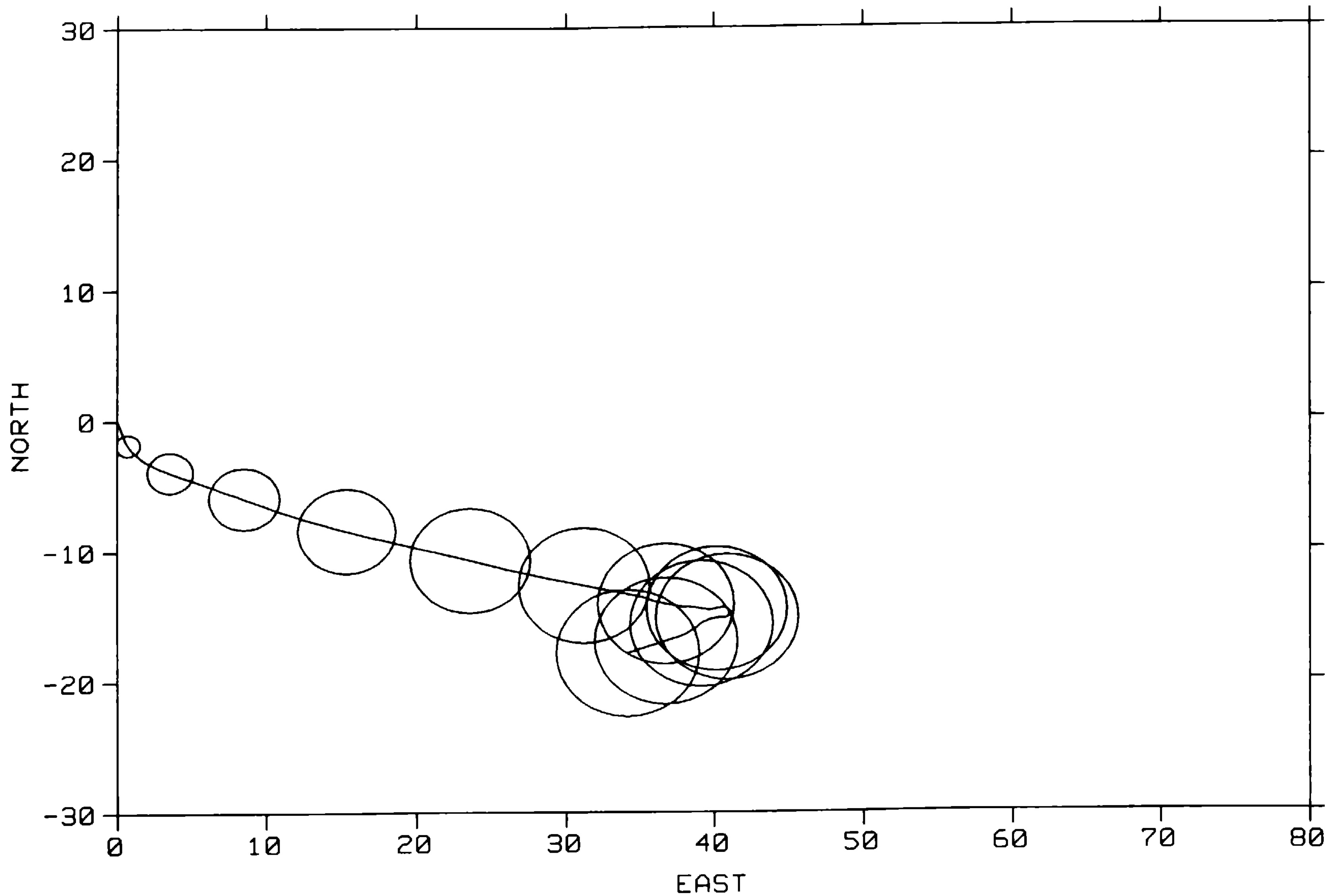

Figure 29. **Balloon trajectory projected on earth surface showing CEP boundaries at 10 minute intervals.** (units = knots) Weather data from San Nicholas Island typical for the month of December.

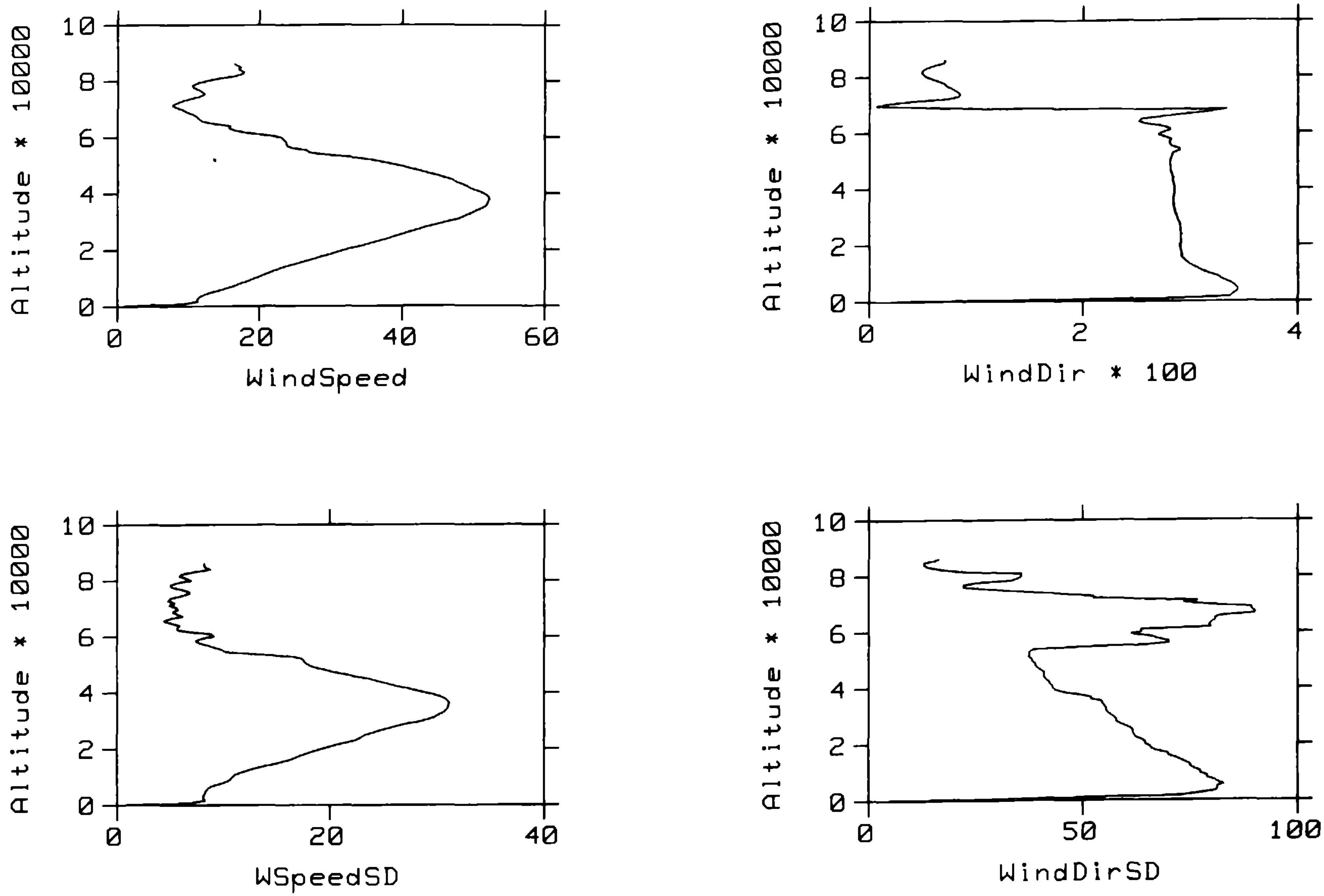

Figure 30. Altitude in feet, wind speed in knots, wind direction in degrees clockwise from North, weather data from San Nicholas Island typical for the month of December.